AD NUMBER

AD907813

LIMITATION CHANGES

TO:

Approved for public release; distribution is unlimited.

FROM:

Distribution authorized to U.S. Gov't. agencies only; Test and Evaluation; FEB 1973. Other requests shall be referred to Air Force Armament Laboratory, Attn: DLGC, Eglin AFB, FL 32542.

AUTHORITY

AFATL ltr, 10 Oct 1975

AEDC-TR-73-37
AFATL-TR-73-29

Cy.2

SEPARATION TRAJECTORIES OF VARIOUS MUNITIONS WHEN RELEASED FROM THE A-7D AIRCRAFT AT MACH NUMBERS FROM 0.33 TO 0.95

David W. Hill, Jr.

ARO, Inc.

February 1973

PROPULSION WIND TUNNEL FACILITY
ARNOLD ENGINEERING DEVELOPMENT CENTER
AIR FORCE SYSTEMS COMMAND
ARNOLD AIR FORCE STATION, TENNESSEE

NOTICES

When U. S. Government drawings specifications, or other data are used for any purpose other than a definitely related Government procurement operation, the Government thereby incurs no responsibility nor any obligation whatsoever, and the fact that the Government may have formulated, furnished, or in any way supplied the said drawings, specifications, or other data, is not to be regarded by implication or otherwise, or in any manner licensing the holder or any other person or corporation, or conveying any rights or permission to manufacture, use, or sell any patented invention that may in any way be related thereto.

Qualified users may obtain copies of this report from the Defense Documentation Center.

References to named commercial products in this report are not to be considered in any sense as an endorsement of the product by the United States Air Force or the Government.

SEPARATION TRAJECTORIES OF VARIOUS MUNITIONS WHEN RELEASED FROM THE A-7D AIRCRAFT AT MACH NUMBERS FROM 0.33 TO 0.95

David W. Hill, Jr.
ARO, Inc.

FOREWORD

The work reported herein was conducted by the Arnold Engineering Development Center (AEDC) and sponsored by the Air Force Armament Laboratory (AFATL/DLGC), Air Force Systems Command (AFSC), under Program Element 27121F, System 337A.

The test results presented were obtained by ARO, Inc. (a subsidiary of Sverdrup & Parcel and Associates, Inc.), contract operator of AEDC, AFSC, Arnold Air Force Station, Tennessee. The test was conducted from September 22 to 28, 1972, under ARO Project No. PA031. The manuscript was submitted for publication on December 21, 1972.

This technical report has been reviewed and is approved.

L. R. KISSLING
Lt Colonel, USAF
Chief Air Force Test Director, PWT
Directorate of Test

A. L. COAPMAN
Colonel, USAF
Director of Test

ABSTRACT

Wind tunnel captive trajectory tests were conducted in the Aerodynamic Wind Tunnel (4T) to investigate the separation characteristics of various external stores from the wing, pylons, and racks of the A-7D aircraft. Separation trajectory data were obtained for the MK-84 LGB, M-84 EOGB, MK-82 LGB, and BLU-1/B bombs, and for the loaded and expended LAU-68 A/A rocket launcher. Trajectories were obtained at Mach numbers from 0.33 to 0.95 at simulated altitudes from 4,000 to 15,000 ft. At selected test conditions, parent-aircraft climb angles of 0 to -70 deg were simulated. In general, the stores separated from the aircraft without contacting the wing, pylon, or rack.

CONTENTS

APPENDIXES

I. ILLUSTRATIONS

Figure

NOMENCLATURE

BL	Aircraft buttock line from plane of symmetry, in., model scale
b	Store reference dimension, ft full scale
C_A	Store axial-force coefficient, axial force/$q_\infty S$
C_ℓ	Store rolling-moment coefficient, rolling moment/$q_\infty Sb$
C_{ℓ_p}	Store roll-damping derivative, $dC_\ell/d(pb/2V_\infty)$
C_m	Store pitching-moment coefficient, referenced to the store cg, pitching moment/$q_\infty Sb$
C_{m_q}	Store pitch-damping derivative, $dC_m/d(qb/2V_\infty)$
C_n	Store yawing-moment coefficient, referenced to the store cg, yawing moment/$q_\infty Sb$
C_{n_r}	Store yaw-damping derivative, $dC_n/d(rb/2V_\infty)$

FS	Aircraft fuselage station, in., model scale
F_Z	MER/TER ejector force, lb
F_{Z_1}	Pylon forward ejector force, lb
F_{Z_2}	Pylon aft ejector force, lb
H	Pressure altitude, ft
I_{xx}	Full-scale moment of inertia about the store X_B axis, slug-ft^2
I_{yy}	Full-scale moment of inertia about the store Y_B axis, slug-ft^2
I_{zz}	Full-scale moment of inertia about the store Z_B axis, slug-ft^2
M_∞	Free-stream Mach number
$\overline{m}$	Full-scale store mass, slugs
p	Store angular velocity about the X_B axis, radians/sec
q	Store angular velocity about the Y_B axis, radians/sec
q_∞	Free-stream dynamic pressure, psf
r	Store angular velocity about the Z_B axis, radians/sec
S	Store reference area, ft^2, full scale
t	Real trajectory time from initiation of trajectory, sec
V_∞	Free-stream velocity, ft/sec
WL	Aircraft waterline from reference horizontal plane, in., model scale
X	Separation distance of the store cg parallel to the flight axis system X_F direction, ft, full scale measured from the prelaunch position
X_{cg}	Full-scale cg location, ft from nose of store
X_L	Ejector piston location relative to the store cg, positive forward of store cg, ft, full scale
X_{L_1}	Forward ejector piston location relative to the store cg, positive forward of store cg, ft, full scale

X_{L_2} Aft ejector piston location relative to the store cg, positive forward of store cg, ft, full scale

Y Separation distance of the store cg parallel to the flight axis system Y_F direction, ft, full scale measured from the prelaunch position

Z Separation distance of the store cg parallel to the flight-axis system Z_F direction, ft, full scale measured from the prelaunch position

Z_E Ejector stroke length, ft, full scale

α Parent-aircraft model angle of attack relative to the free-stream velocity vector, deg

θ Angle between the store longitudinal axis and its projection in the X_F-Y_F plane, positive when store nose is raised as seen by pilot, deg

$\bar{\theta}$ Simulated parent-aircraft climb angle. Angle between the flight direction and the earth horizontal, deg, positive for increasing altitude

ϕ Angle between the projection of the store lateral axis in the Y_F-Z_F plane and the Y_F axis, positive for clockwise rotation when looking upstream, deg

ψ Angle between the projection of the store longitudinal axis in the X_F-Y_F plane and the X_F axis, positive when the store nose is to the right as seen by the pilot, deg

FLIGHT-AXIS SYSTEM COORDINATES

Directions

X_F Parallel to the free-stream wind vector, positive direction is forward as seen by the pilot

Y_F Perpendicular to the X_F and Z_F directions, positive direction is to the right as seen by the pilot

Z_F In the aircraft plane of symmetry, perpendicular to the free-stream wind vector, positive direction is downward

The flight-axis system origin is coincident with the aircraft cg and remains fixed with respect to the parent aircraft during store separation. The X_F, Y_F, and Z_F coordinate axes do not rotate with respect to the initial flight direction and attitude.

STORE BODY-AXIS SYSTEM COORDINATES

Directions

X_B Parallel to the store longitudinal axis, positive direction is upstream in the prelaunch position

Y_B Perpendicular to the store longitudinal axis, and parallel to the flight-axis system X_F-Y_F plane when the store is at zero roll angle, positive direction is to the right looking upstream when the store is at zero yaw and roll angles

Z_B Perpendicular to both the X_B and Y_B axes, positive direction is downward as seen by the pilot when the store is at zero pitch and roll angles.

The store body-axis system origin is coincident with the store cg and moves with the store during separation from the parent airplane. The X_B, Y_B, and Z_B coordinate axes rotate with the store in pitch, yaw, and roll so that mass moments of inertia about the three axes are not time-varying quantities.

SECTION I
INTRODUCTION

A captive trajectory test was conducted in the Aerodynamic Wind Tunnel (4T) to determine the separation characteristics of the MK-84 LGB, MK-84 EOGB, MK-82 LGB, and BLU-1/B bombs and the LAU-68 A/A rocket launcher. All separation trajectories were initiated from the carriage position with simulated ejector forces acting on the stores.

To simulate the separation trajectories, 0.05-scale models of the A-7D aircraft and the various stores were employed. The flight conditions simulated were Mach numbers from 0.33 to 0.95 and altitudes from 4,000 to 15,000 ft. At selected test conditions parent aircraft climb angles of 0 to -70 deg were simulated.

The separation trajectories were initiated from all three pylon stations on the left and right wings of the aircraft model. The ejector forces used were constant values acting throughout the time of piston extension, and were supplied by the sponsoring AFATL office.

SECTION II
APPARATUS

2.1 TEST FACILITY

The Aerodynamic Wind Tunnel (4T) is a closed-loop, continuous flow, variable-density tunnel in which the Mach number can be varied from 0.1 to 1.3. At all Mach numbers, the stagnation pressure can be varied from 300 to 3700 psfa. The test section is 4 ft square and 12.5 ft long with perforated, variable porosity (0.5- to 10-percent open) walls. It is completely enclosed in a plenum chamber from which the air can be evacuated, allowing part of the tunnel airflow to be removed through the perforated walls of the test section. A more thorough description of the tunnel is given in the Test Facilities Handbook.[1]

For store separation testing, two separate and independent support systems are used to support the models. The parent aircraft model is inverted in the test section and supported by an offset sting attached to the main pitch sector. The store model is supported by the captive trajectory support (CTS) which extends down from the tunnel top wall and provides store movement (six degrees of freedom) independent of the parent-aircraft model. An isometric drawing of a typical store separation installation is shown in Fig. 1, Appendix I.

Also shown in Fig. 1 is a block diagram of the computer control loop used during captive trajectory testing. The analog system and the digital computer work as an integrated

---

[1]Test Facilities Handbook (Ninth Edition). "Propulsion Wind Tunnel Facility, Vol. 4." Arnold Engineering Development Center, July 1971.

unit and, utilizing required input information, control the store movement during a trajectory. Store positioning is accomplished by use of six individual d-c electric motors. Maximum translational travel of the CTS is ±15 in. from the tunnel centerline in the lateral and vertical directions and 36 in. in the axial direction. Maximum angular displacements are ±45 deg in pitch and yaw and ±360 deg in roll. A more complete description of the test facility can be found in the Test Facilities Handbook. A schematic showing the test section details and the location of the models in the tunnel is shown in Fig. 2.

2.2 TEST ARTICLES

The test articles used were 0.05-scale models of the stores and the A-7D aircraft (including pylons, racks, and models used for configuration loading). The A-7D model was geometrically similar to the full-scale airplane except for some modifications incident to the wind tunnel installation and CTS operation. A sketch of the A-7D model showing basic dimensions and location of the wing pylon stations is shown in Fig. 3. Dimensions of the wing pylons are presented in Fig. 4. When installed on the aircraft, all pylon surfaces for store and rack mounting are at a 3-deg nose down attitude with respect to the aircraft waterline. Triple ejection rack (TER) and multiple ejection rack (MER) details are shown in Figs. 5 and 6. These racks were mounted on the pylons at a position corresponding to the 30-in. lug attachment.

Details and dimensions of the MK-84 LGB, MK-84 EOGB, MK-82 LGB, loaded and expended LAU-68 A/A, BLU-1/B, 300-gal fuel tank, M-117 GP, MK-20, CBU-24, and CBU-38 are shown in Figs. 7 through 17, respectively.

The A-7D aircraft model was inverted in the tunnel and attached by an offset sting to the main sting-support system. Store models were mounted on an internal strain-gage balance that was attached to the CTS system. A photograph showing a typical A-7D CTS installation in the tunnel is shown in Fig. 18.

2.3 INSTRUMENTATION

Two internal strain-gage balances were used during the test. A 0.40-in.-diam, 6-component balance was used for tests with the MK-84 LGB, MK-84 EOGB, and BLU-1; and a 0.16-in.-diam, 5-component balance was used for tests with the MK-82 LGB and LAU-68 A/A (loaded and expended). Translational and angular positions of the store models were obtained from the CTS analog outputs. The aircraft angle of attack was set using the main sting support and digital readout system. The pylons and racks were instrumented with spring-loaded plungers (touch wires) which were electrically connected to give a visual indication on the control console when the store contacted the touch wire at the carriage position. The CTS system was also electrically connected to automatically stop the CTS movement if the store model or CTS contacted the aircraft model, aircraft support sting, or the test section walls.

SECTION III
TEST DESCRIPTION

3.1 TEST CONDITIONS

Separation trajectory data were obtained at Mach numbers from 0.33 to 0.95. Tunnel dynamic pressure ranged from 240 psf at M_∞ = 0.33 to 500 psf at M_∞ = 0.95, and tunnel stagnation temperature was maintained near 100°F.

Tunnel conditions were held constant at the desired Mach number and stagnation pressure while data for each trajectory were obtained. The trajectories were terminated when the store or sting contacted the parent-aircraft model or when a CTS limit was reached.

3.2 TRAJECTORY DATA ACQUISITION

To obtain a trajectory, test conditions were established in the tunnel and the parent model was positioned at the desired angle of attack. The store model was then oriented to a position corresponding to the store carriage location. After the store was set at the desired initial position, operational control of the CTS was switched to the digital computer which controlled the store movement during the trajectory through commands to the CTS analog system (see block diagram, Fig. 1). Data from the wind tunnel, consisting of measured model forces and moments, wind tunnel operating conditions, and CTS rig positions, were input to the digital computer for use in the full-scale trajectory calculations.

The digital computer was programmed to solve the six-degree-of-freedom equations to calculate the angular and linear displacements of the store relative to the parent aircraft pylon. In general, the program involves using the last two successive measured values of each static aerodynamic coefficient to predict the magnitude of the coefficients over the next time interval of the trajectory. These predicted values are used to calculate the new position and attitude of the store at the end of the time interval. The CTS is then commanded to move the store model to this new position and the aerodynamic loads are measured. If these new measurements agree with the predicted values, the process is continued over another time interval of the same magnitude. If the measured and predicted values do not agree within the desired precision, the calculation is repeated over a time interval one-half the previous value. This process is repeated until a complete trajectory has been obtained.

In applying the wind tunnel data to the calculations of the full-scale store trajectories, the measured forces and moments are reduced to coefficient form and then applied with proper full-scale store dimensions and flight dynamic pressure. Dynamic pressure was calculated using a flight velocity equal to the free-stream velocity component plus the components of store velocity relative to the aircraft, and a density corresponding to the simulated altitude.

The initial portion of each launch trajectory incorporated simulated ejector forces in addition to the measured aerodynamic forces acting on the store. For all trajectories, the ejector force was simulated using a constant force applied throughout the time interval when the ejector piston was extending to its maximum stroke. Identification of the ejector forces used for the stores is presented in Table I (Appendix II). The ejector force was considered to act perpendicular to the (rack or pylon) mounting surface. The locations of the applied ejector forces and other full-scale store parameters used in the trajectory calculations are listed in Table II.

3.3 CORRECTIONS

Balance, sting, and support deflections caused by the aerodynamic loads on the store models were accounted for in the data reduction program to calculate the true store-model angles. Corrections were also made for model weight tares to calculate the net aerodynamic forces on the store model.

3.4 PRECISION OF DATA

The trajectory data are subject to error resulting from uncertainties in tunnel conditions, balance measurements, extrapolation tolerances, and CTS positioning control. Maximum uncertainty in the CTS position control was ±0.05 in. for translational settings and ±0.15 deg for angular displacements in pitch and yaw. Extrapolation tolerances were ±0.1 for all aerodynamic coefficients. Based on a 95-percent confidence level, and ignoring bias errors, the uncertainties in the full-scale trajectory data resulting from balance precision limitations were calculated and are presented in Table III.

Estimated uncertainty in setting Mach number was ±0.003, and the uncertainty in aircraft model angle of attack was estimated to be ±0.1 deg.

SECTION IV
RESULTS AND DISCUSSION

Separation trajectory data were obtained for the MK-84 LGB, MK-84 EOGB, MK-82 LGB, LAU-68 A/A, and BLU-1/B stores when ejected from the A-7D aircraft. Data showing the linear displacements of the store cg relative to the carriage position and the angular displacements relative to the flight-axis coordinate system are presented as functions of full-scale trajectory time. Positive X, Y, and Z displacements (as seen by the pilot) are forward, to the right, and down, respectively. Positive changes in θ, ψ, and ϕ (as seen by the pilot) are nose up, nose right, and clockwise, respectively. Identification of the simulated ejector forces used during the test is given in Table I, and full-scale store parameters used in the trajectory calculations are presented in Table II. Note that the axial-force coefficient was an input parameter for the MK-82 LGB and LAU-68 A/A stores. This was necessary because the internal balance used during testing of these models did not have an axial-force gage. The axial-force coefficients used were estimated from existing data on similar models.

Aircraft wing-loading configurations are identified in Table IV. Identification of the TER and MER stations used in Table IV is given in Fig. 19. Note that the combined wing-loading configurations for the left and right wings were for convenience of testing in the wind tunnel.

In general, all stores separated from the aircraft without contacting the wing, pylon, or rack.

4.1 MK-84 LGB AND MK-84 EOGB DATA

Separation trajectory data obtained for the MK-84 LGB and MK-84 EOGB stores are presented in Figs. 20 and 21, respectively. These data show the trajectories for the stores at Mach number/angle-of-attack combinations representing various climb angles and simulated altitudes. At the lowest Mach number (M_∞ = 0.33), very little pitch motion is seen as compared to the nose-down pitch motion occurring at the higher Mach numbers.

The presence of adjacent stores produced a significant effect on the MK-84 LGB translational and angular motions (comparing configurations 1R and 2R) for all the Mach numbers. Smaller effects were noted for the MK-84 EOGB (configurations 3R and 4R).

4.2 MK-82 LGB DATA

Trajectory data were obtained for the MK-82 LGB store from both the pylon and MER and are presented in Fig. 22. In general, there was little effect of Mach number on the translational motion of the store from any pylon station. However, increasing the Mach number resulted in increased nose-down pitch motion and nose-outboard yaw motion.

In general, when the MK-82 LGB store was separated from MER Station No. 1 (configurations 8L and 9L), the yawed nose-outboard store for all Mach numbers. The store pitched nose-down in configuration 8L and pitched nose-up in configuration 9L for Mach number 0.95 and $\bar{\theta}$ = -70 deg. Separation of the store from MER Station No. 6 (configurations 8R and 9R) resulted in a "flying motion" (decreasing Z displacement) for trajectory times greater than 0.2 sec at M_∞ = 0.95 and $\bar{\theta}$ = -70 deg.

4.3 LAU-68 A/A DATA

Trajectory data for the loaded and expended LAU-68 A/A stores are presented in Figs. 23 and 24, respectively. Separation characteristics for the loaded and expended stores were similar, with angular motions somewhat greater for the expended store (in part due to its smaller moments of inertia). In general, both stores showed a nose-down pitch motion and a nose-outboard yaw motion.

4.4 BLU-1/B DATA

Separation trajectory data for the BLU-1/B store are presented in Fig. 25. The store was separated from MER Station No. 4 (configuration 12L) and MER Station No. 1 (configuration 12R) at climb angles of -50 and 0 deg, respectively. The changes seen may as well be due to the climb angle as to the different position on the rack. Release from the forward outboard shoulder station while in a 50-deg dive resulted in a nose-outboard yaw motion and a slight nose-down pitch. Release from the aft bottom station while in level flight resulted in nose-up pitch with essentially no yaw. Translational motions and roll showed only small differences.

APPENDIXES

I. ILLUSTRATIONS
II. TABLES

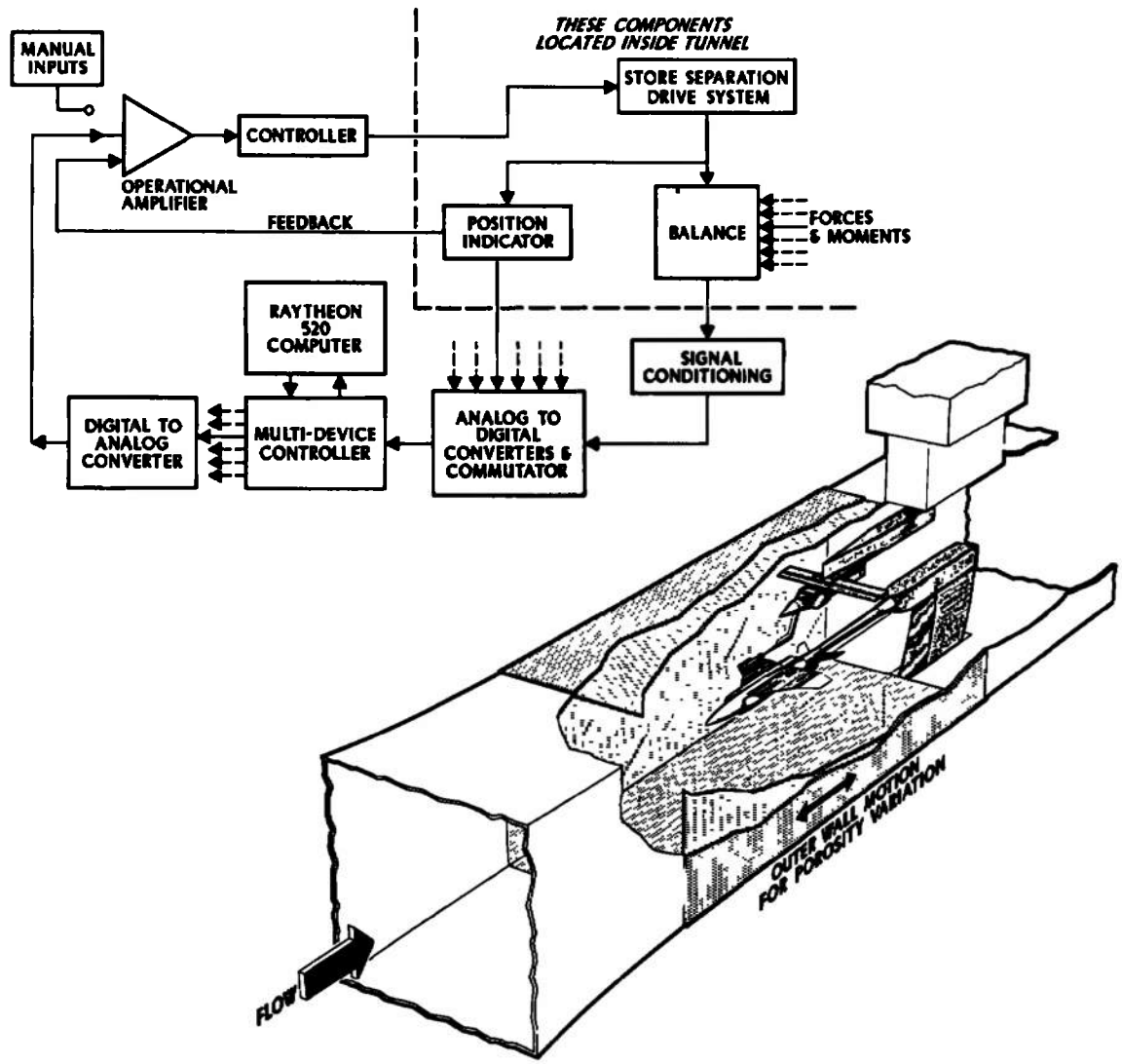

Fig. 1 Isometric Drawing of a Typical Store Separation Installation and a Block Diagram of the Computer Control Loop

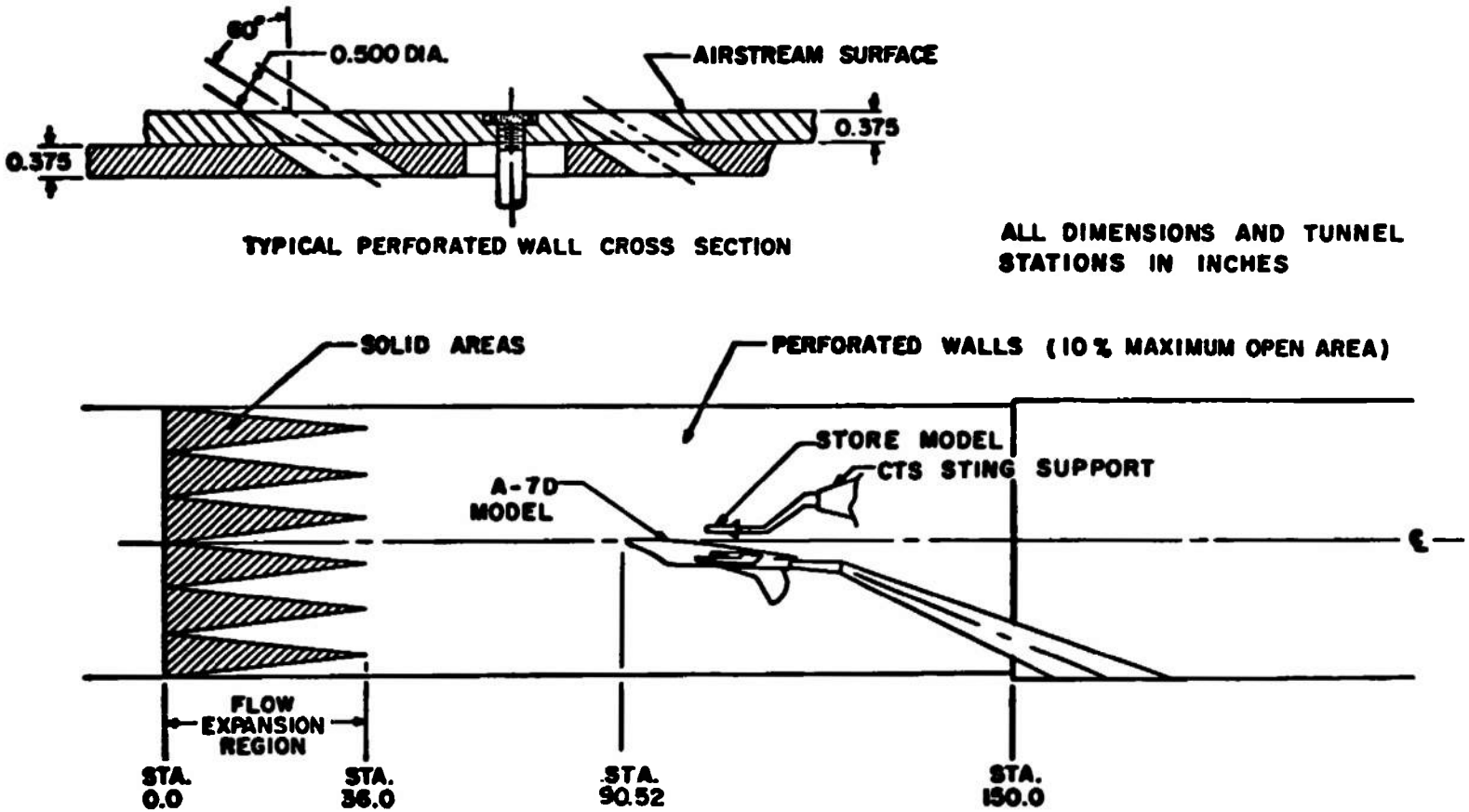

Fig. 2 Schematic of the Tunnel Test Section Showing Model Location

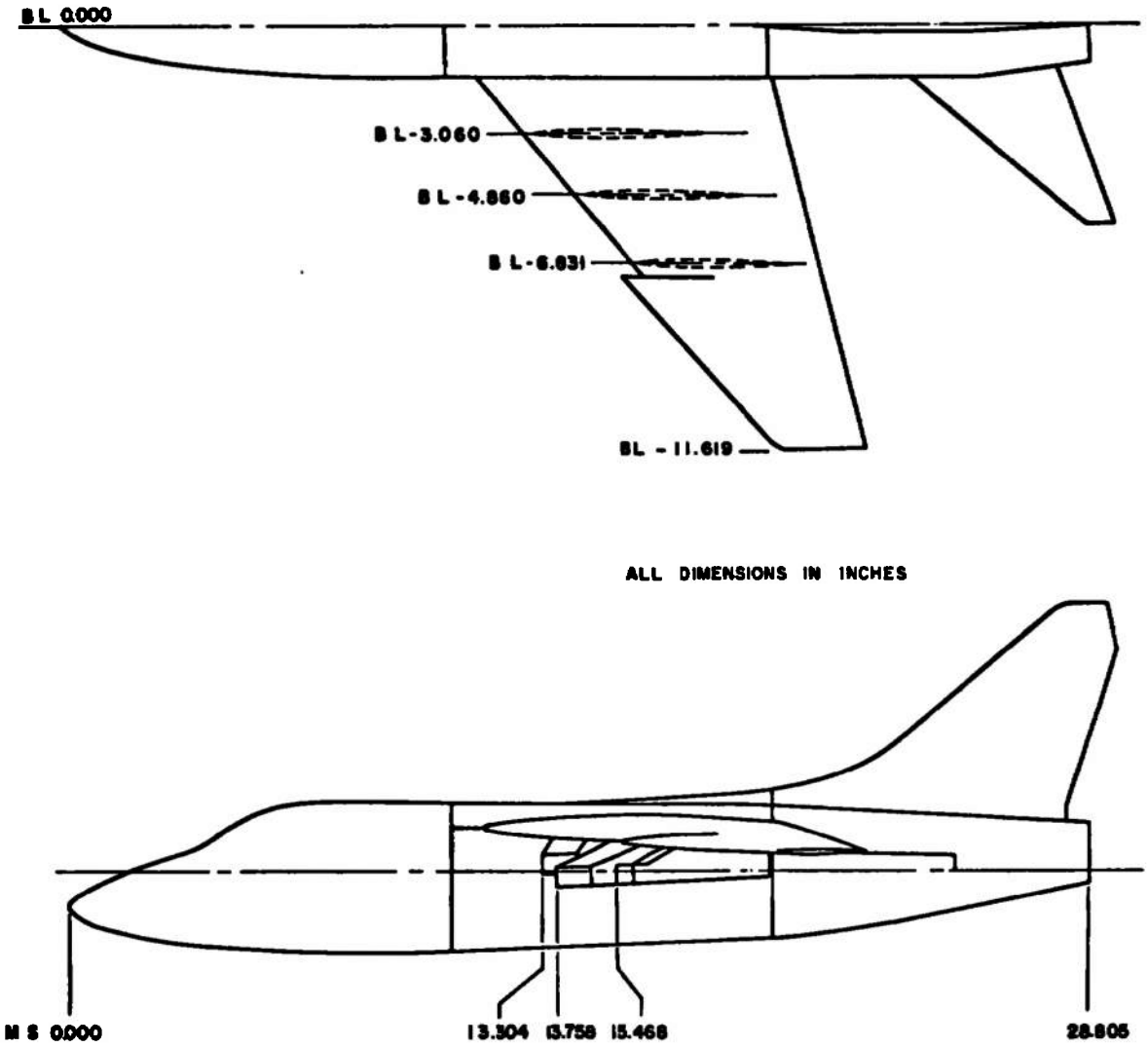

Fig. 3 Sketch of the A-7D Aircraft Model

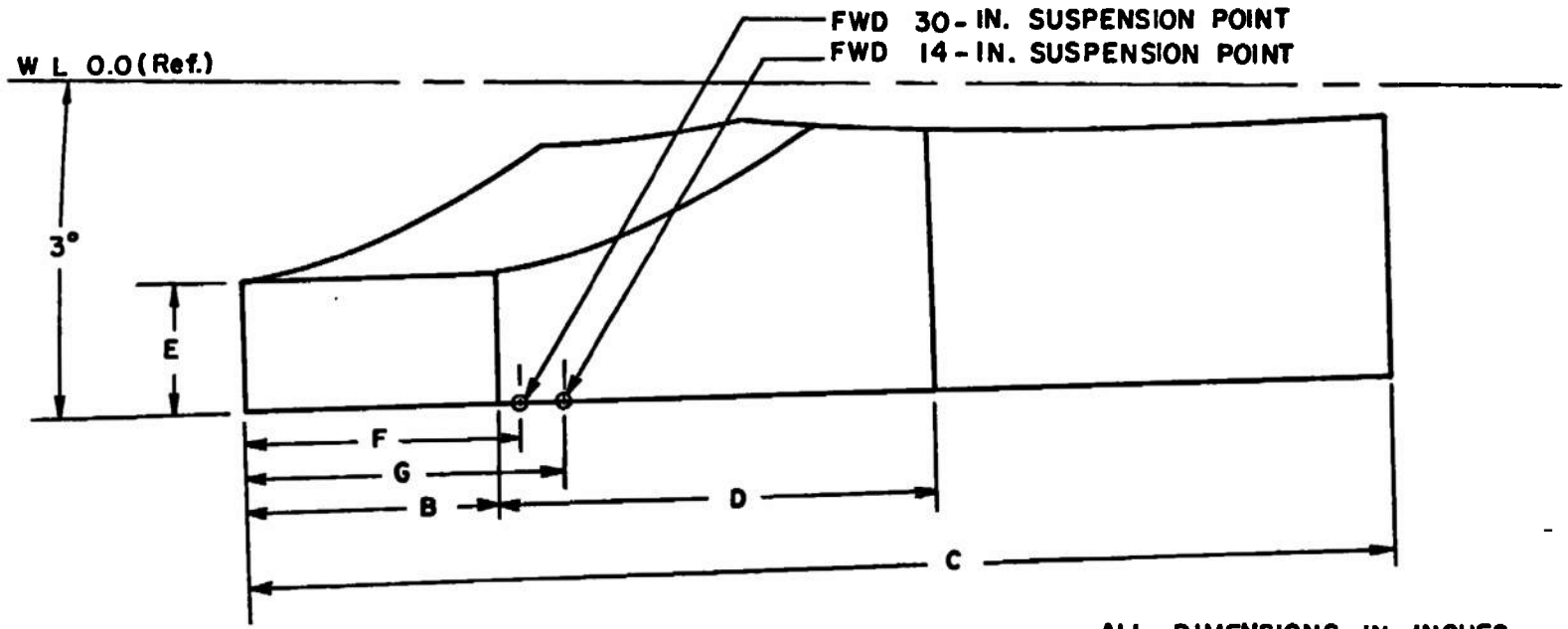

ALL DIMENSIONS IN INCHES

	INBOARD	CENTER	OUTBOARD
B	1.030	1.030	0.515
C	4.580	4.850	4.437
D	1.630	1.905	2.008
E	0.575	0.575	0.513
F	0.950	0.950	0.750
G	1.350	1.350	1.150

Fig. 4 Details and Dimensions of the A-7D Wing Pylon Models

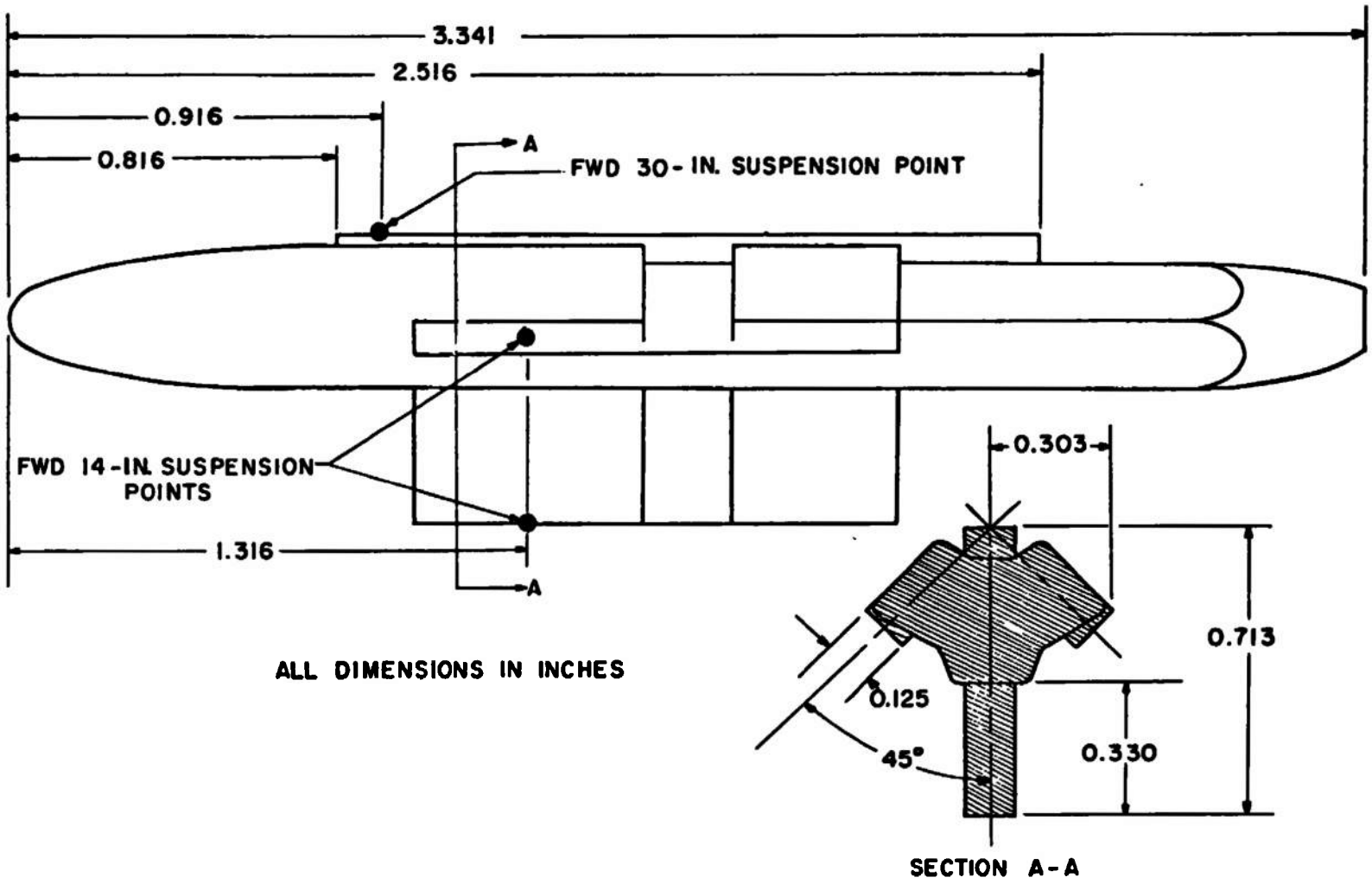

Fig. 5 Details and Dimensions of the TER-9/A Model

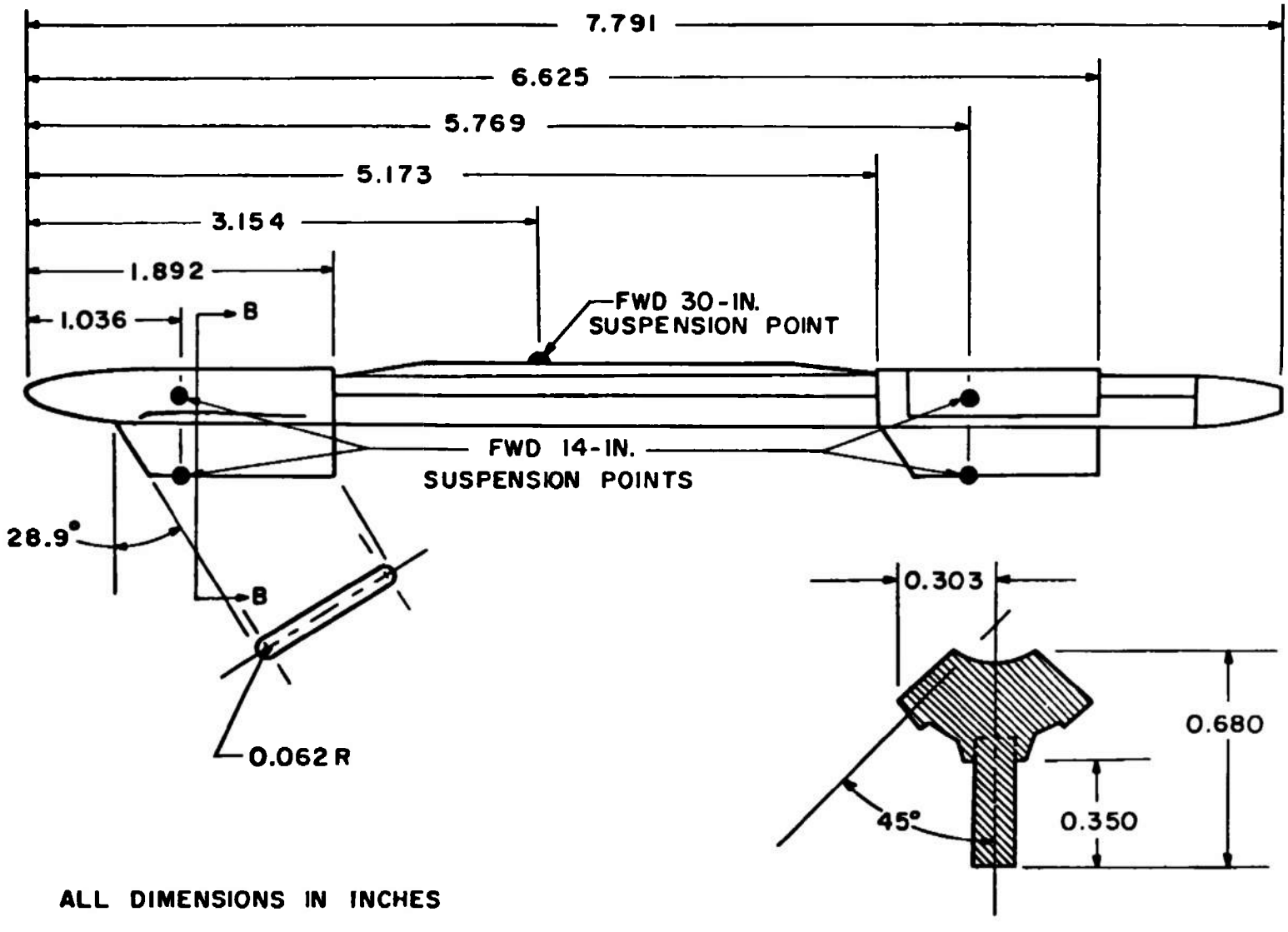

Fig. 6 Details and Dimensions of the MER-ION Model

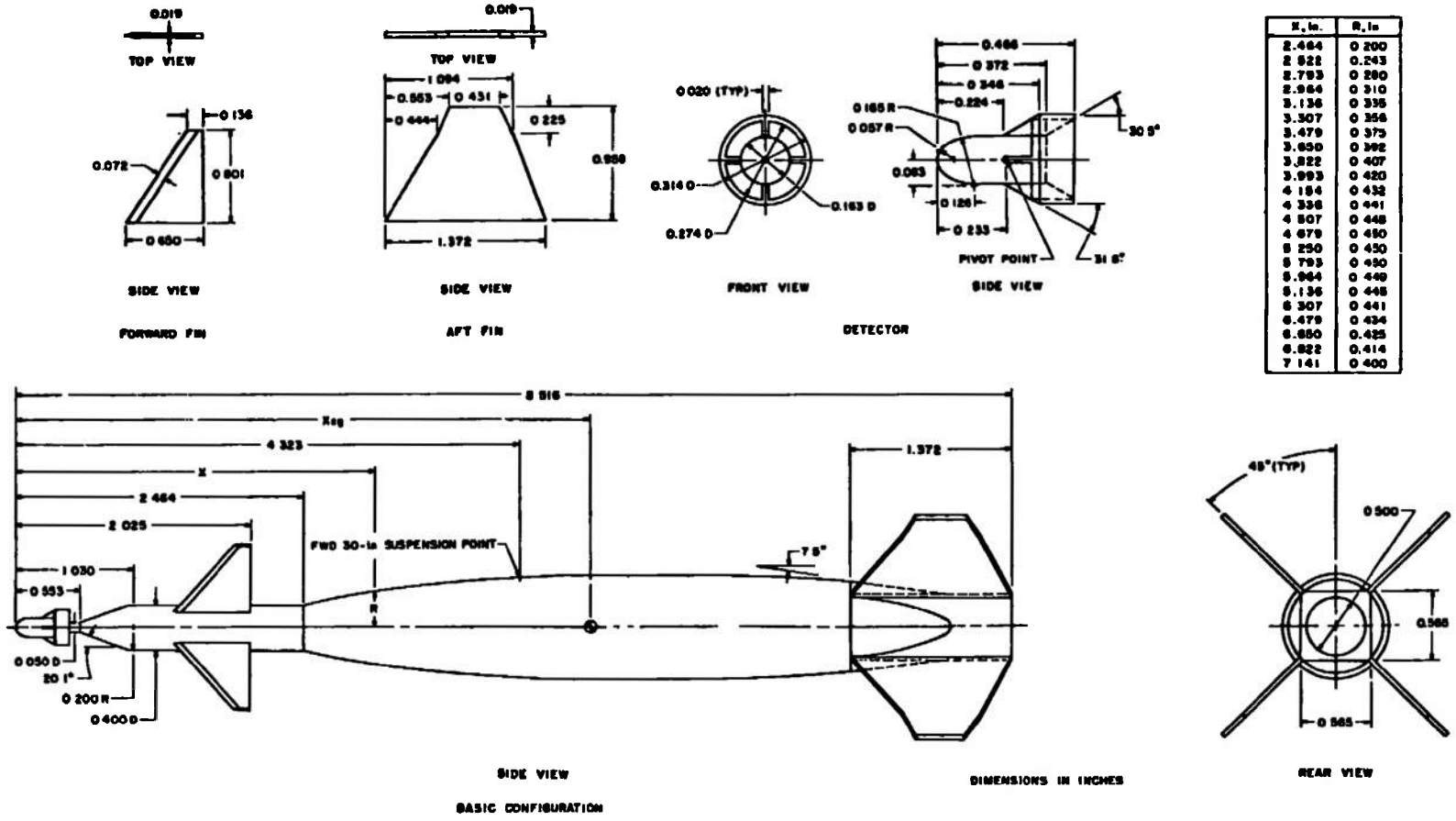

X, in.	R, in.
2.464	0.200
2.522	0.243
2.793	0.280
2.964	0.310
3.136	0.335
3.307	0.356
3.479	0.375
3.650	0.392
3.822	0.407
3.993	0.420
4.164	0.432
4.336	0.441
4.507	0.448
4.679	0.450
5.250	0.450
5.793	0.450
5.964	0.449
6.136	0.445
6.307	0.441
6.479	0.434
6.650	0.425
6.822	0.414
7.141	0.400

Fig. 7 Details and Dimensions of the MK-84 LGB Model

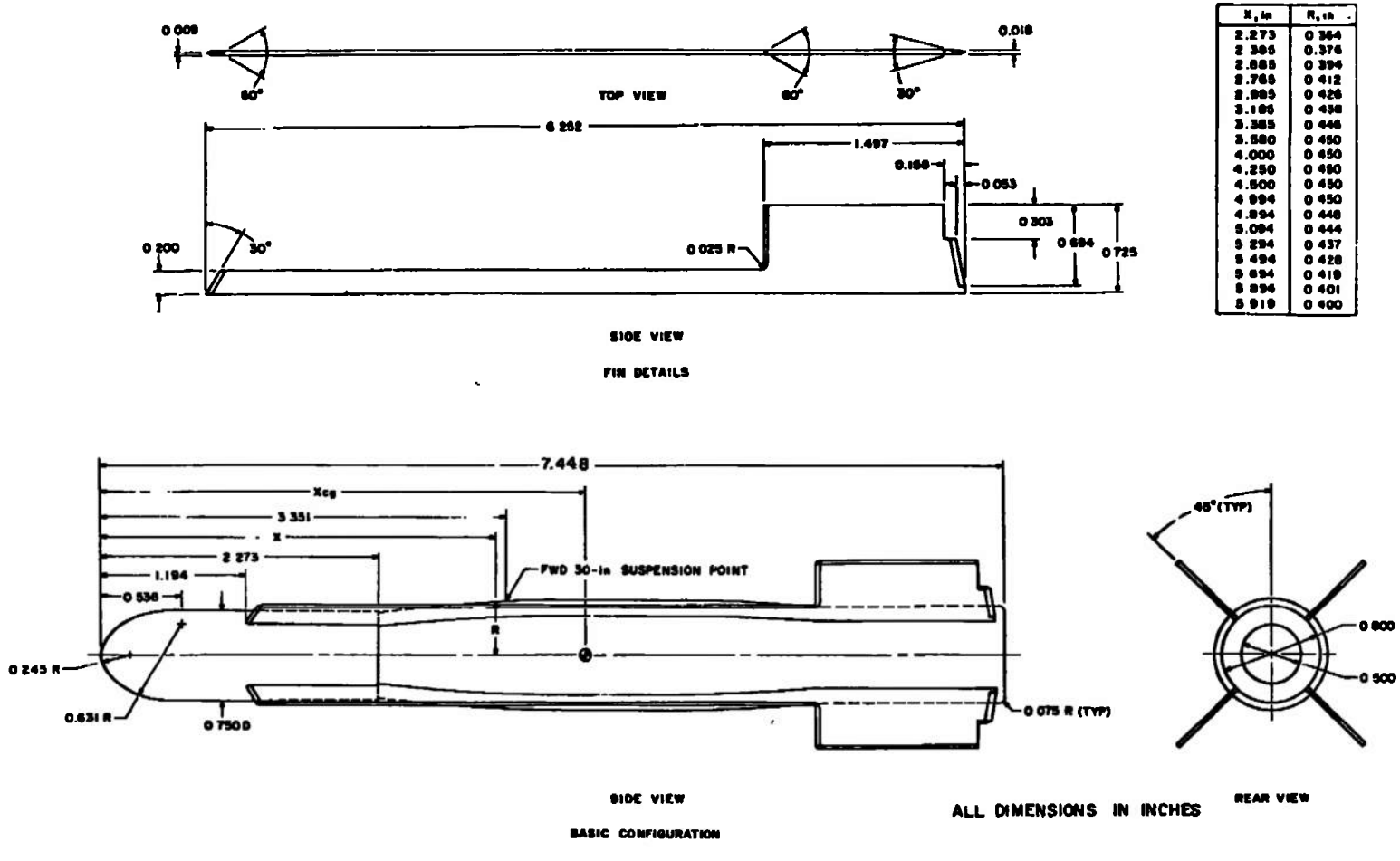

X, in	R, in
2.273	0.364
2.365	0.376
2.665	0.394
2.765	0.412
2.965	0.426
3.165	0.438
3.365	0.446
3.580	0.450
4.000	0.450
4.250	0.450
4.500	0.450
4.994	0.450
4.894	0.446
5.094	0.444
5.294	0.437
5.494	0.428
5.694	0.419
5.894	0.401
5.919	0.400

Fig. 8 Details and Dimensions of the MK-84 EOGB Model

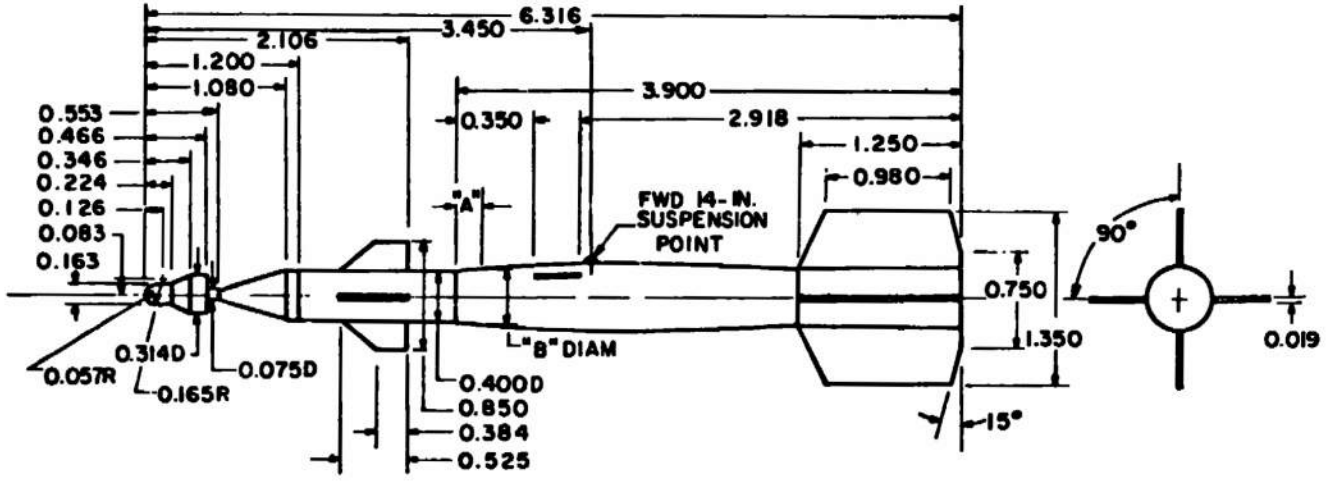

ALL DIMENSIONS IN INCHES

"A"	"B"
0.062	0.421
0.162	0.445
0.262	0.465
0.362	0.483
0.462	0.497
0.562	0.510
0.662	0.520
0.762	0.525
0.862	0.530
0.962	0.532
1.062	0.533
1.162	0.535
1.262	0.537
1.662	0.537
1.762	0.535
1.862	0.525
1.962	0.520
2.062	0.510
2.162	0 497
2.262	0.483
2.362	0.465
2.523	0.438
2.650	0.414

Fig. 9 Details and Dimensions of the MK-82 LGB Model

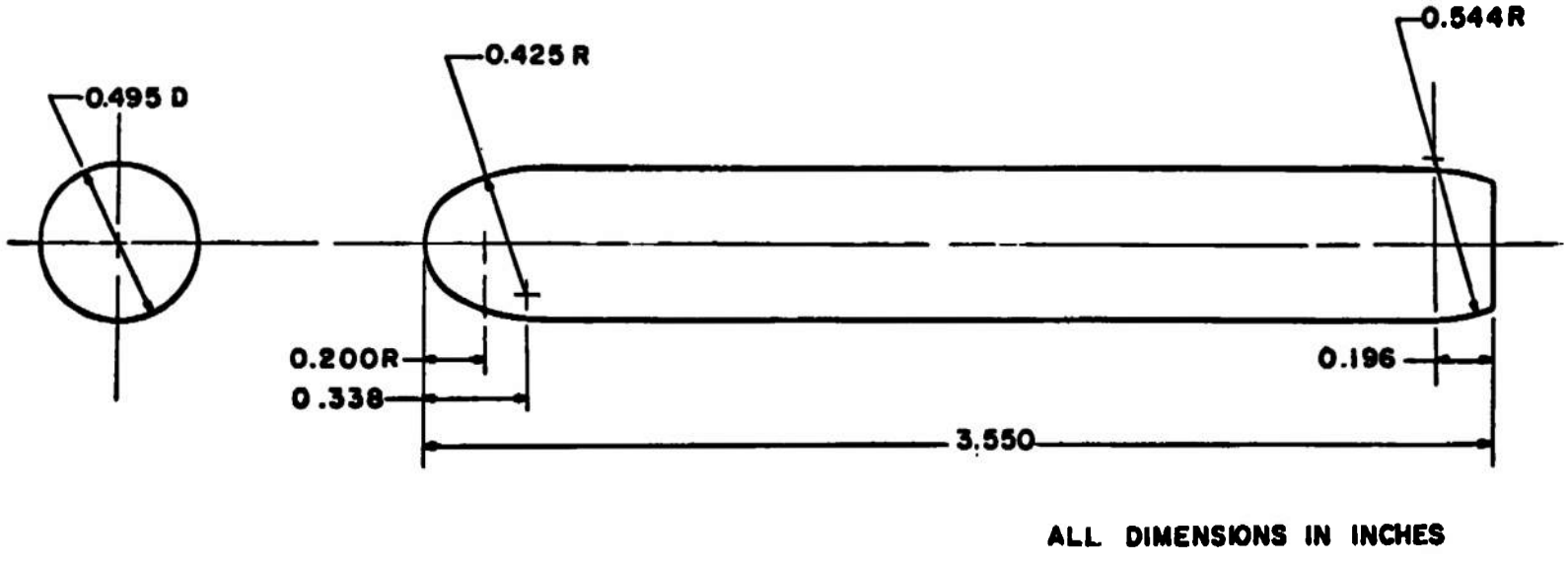

Fig. 10 Details and Dimensions of the Loaded LAU-68 A/A

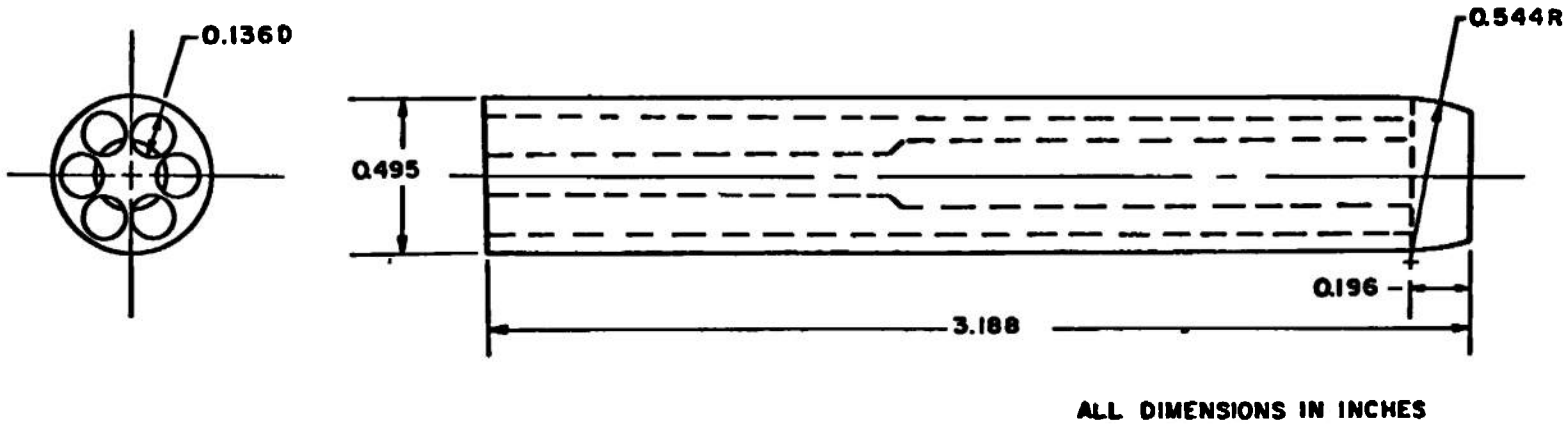

Fig. 11 Details and Dimensions of the Expended LAU-68 A/A Model

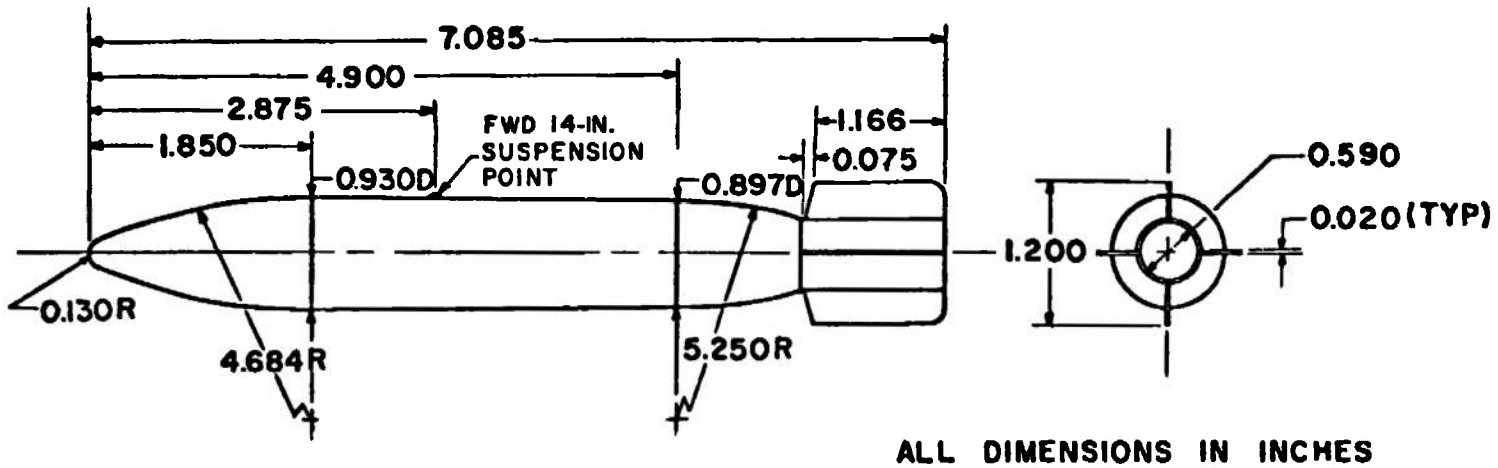

Fig. 12 Details and Dimensions of the Finned BLU-1/B Model

ORDINATES

MODEL STA "X"	RADIUS "R"	MODEL STA "X"	RADIUS "R"
0 000	0 0000	2 250	0.5531
0 060	0 0000	2 500	0 5777
0 100	0 0511	2.750	0 5989
0 150	0 0751		CONSTANT SLOPE
0.200	0 0981	3.450	0 6625
0 250	0 1203		CONSTANT DIAM
0 300	0 1415	6.638	0 6625
0 350	0 1619		CONSTANT SLOPE
0400	0 1815	7.713	0 5680
0 450	0.2003	7.763	0.5637
0 500	0 2183	8 013	0.5409
0 550	0 2355	8 263	0.5162
0 600	0 2521	8 513	0.4899
0 650	0.2680	8.763	0.4620
0.700	0 2833	9.013	0 4327
0 750	0 2979	9.113	0 4206
0 800	0 3119		CONSTANT SLOPE
0 850	0 3253	10 900	0.1815
0 900	0.3383	10.950	0.1733
1.000	0 3625	11.000	0 1646
1.250	0 4153	11 100	0.1441
1 500	0.4587	11 200	0 1170
1.750	0.4950	11.300	0.0725
2 000	0 5260	11.350	0.0000

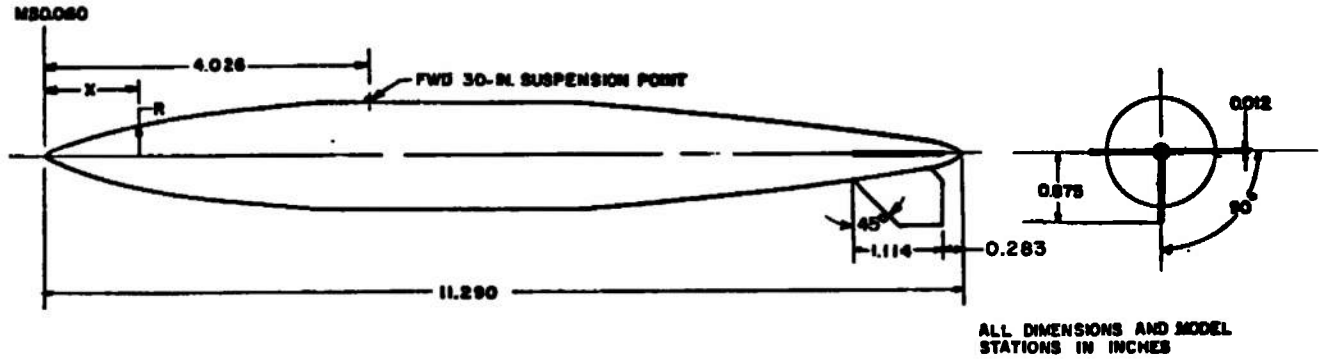

Fig. 13 Details and Dimensions of the 300-gal Fuel Tank Model

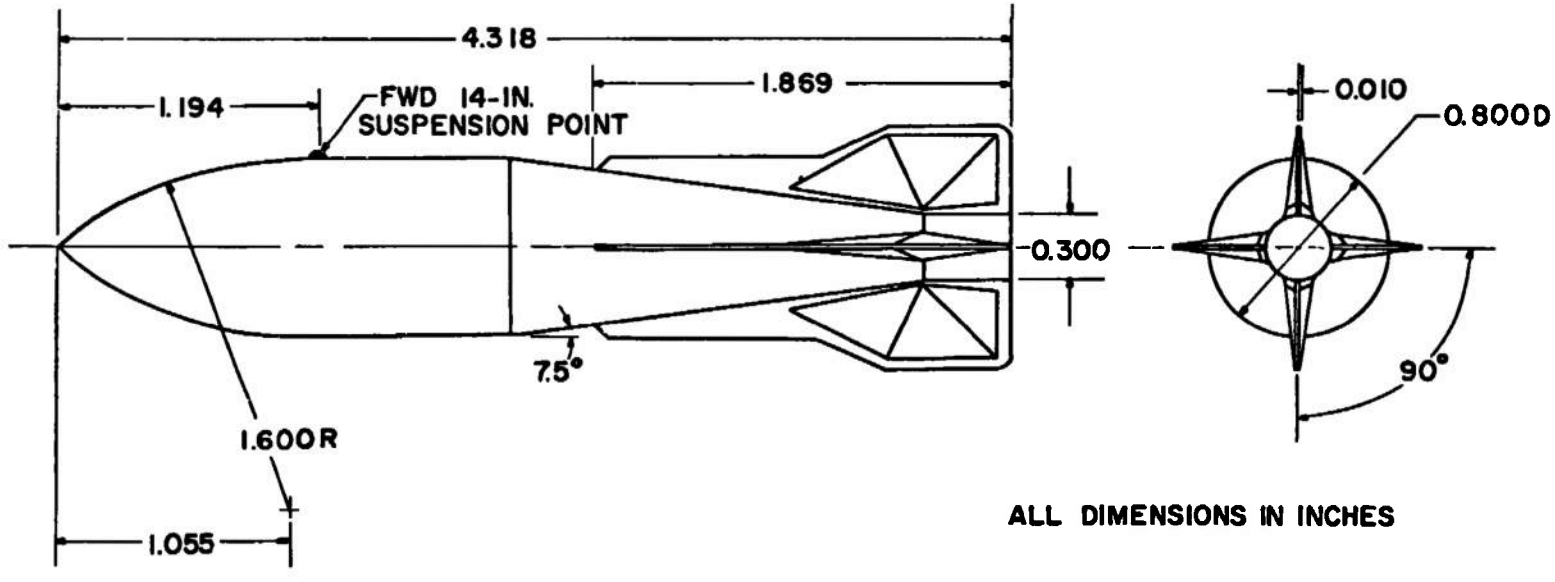

Fig. 14 Details and Dimensions of the M-117 GP Model

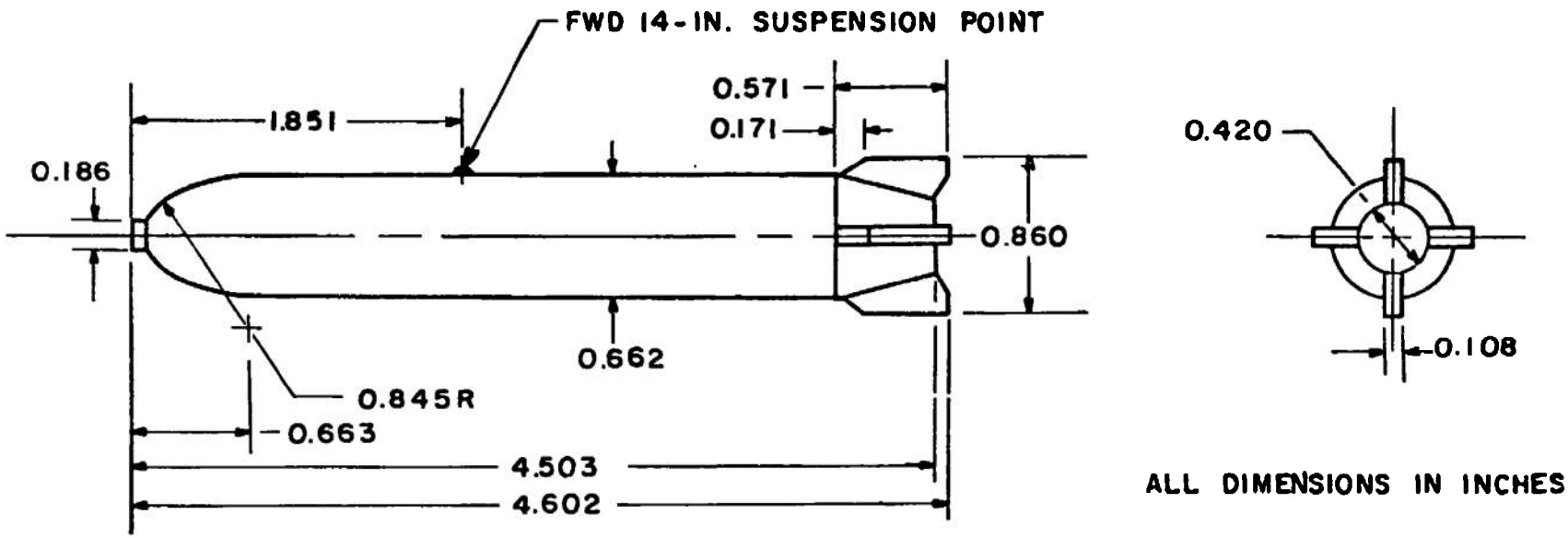

Fig. 15 Details and Dimensions of the MK-20 Model

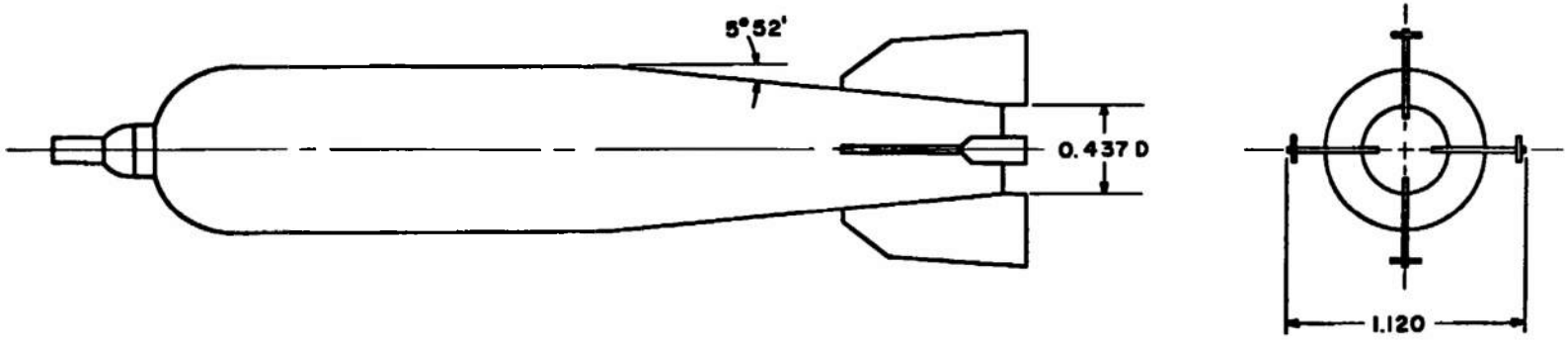

Fig. 16 Details and Dimensions of the CBU-24 Model

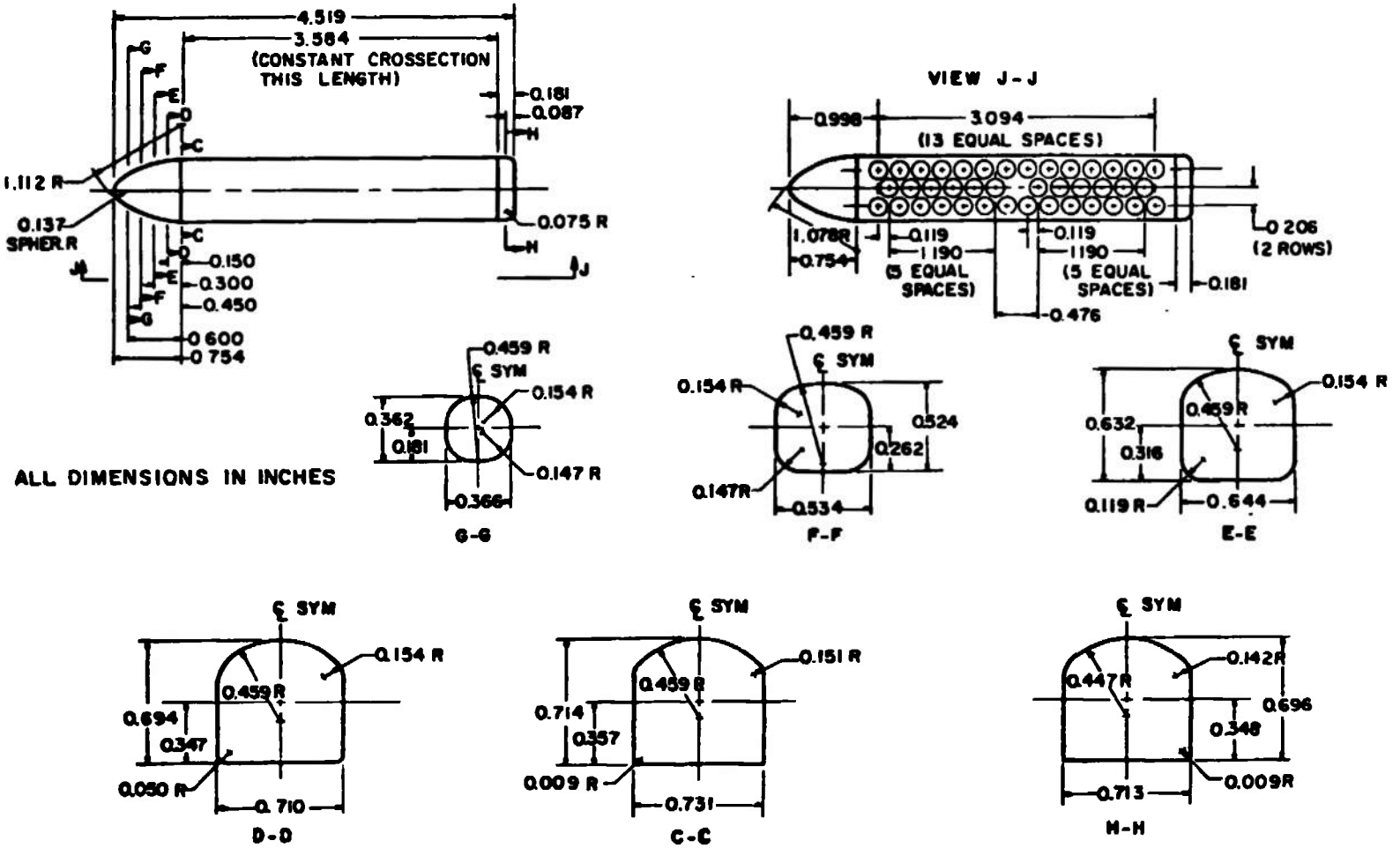

Fig. 17 Details and Dimensions of the CBU-39 Model

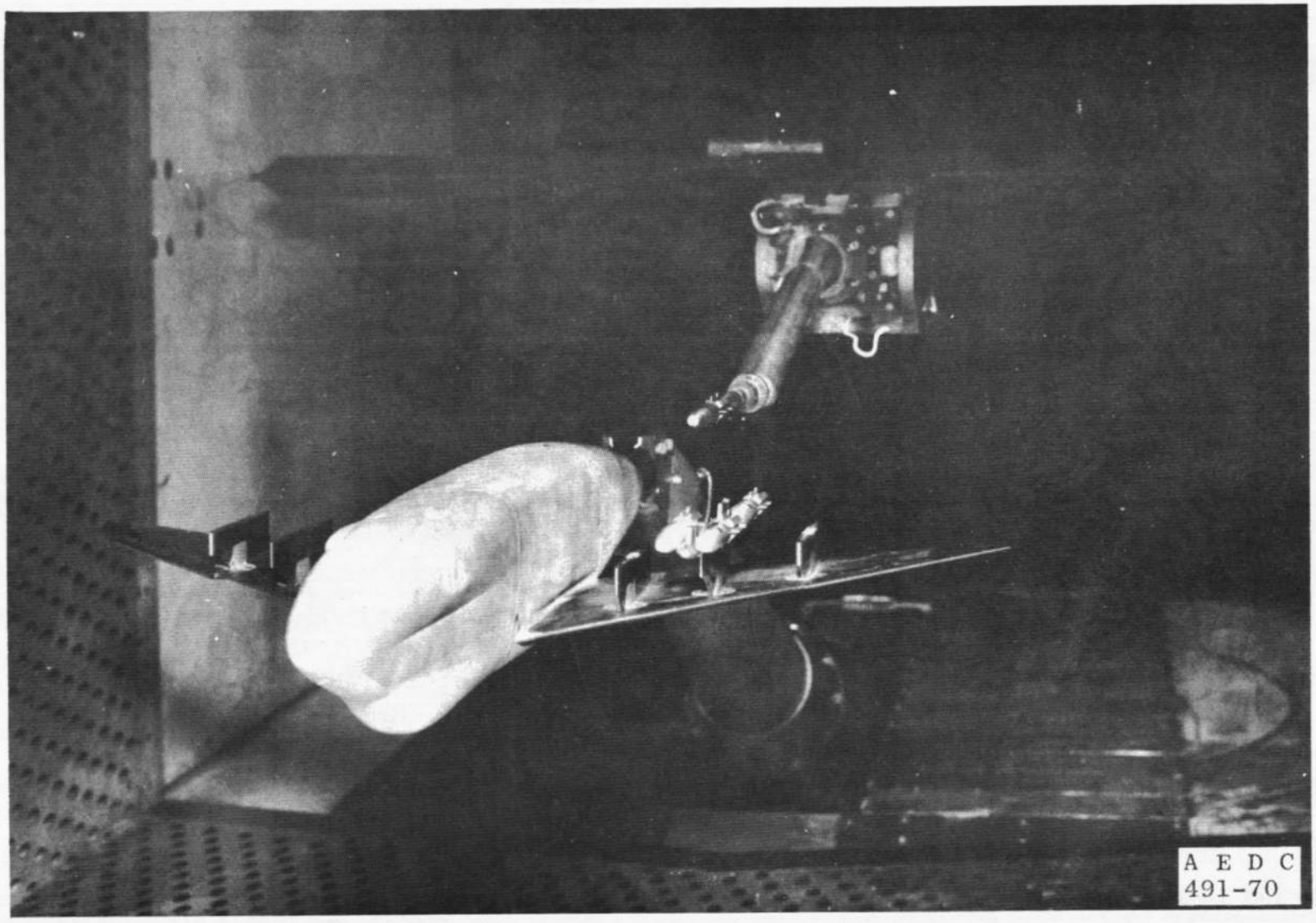

Fig. 18 Photograph of a Typical A-7D CTS Test Installation in the Tunnel

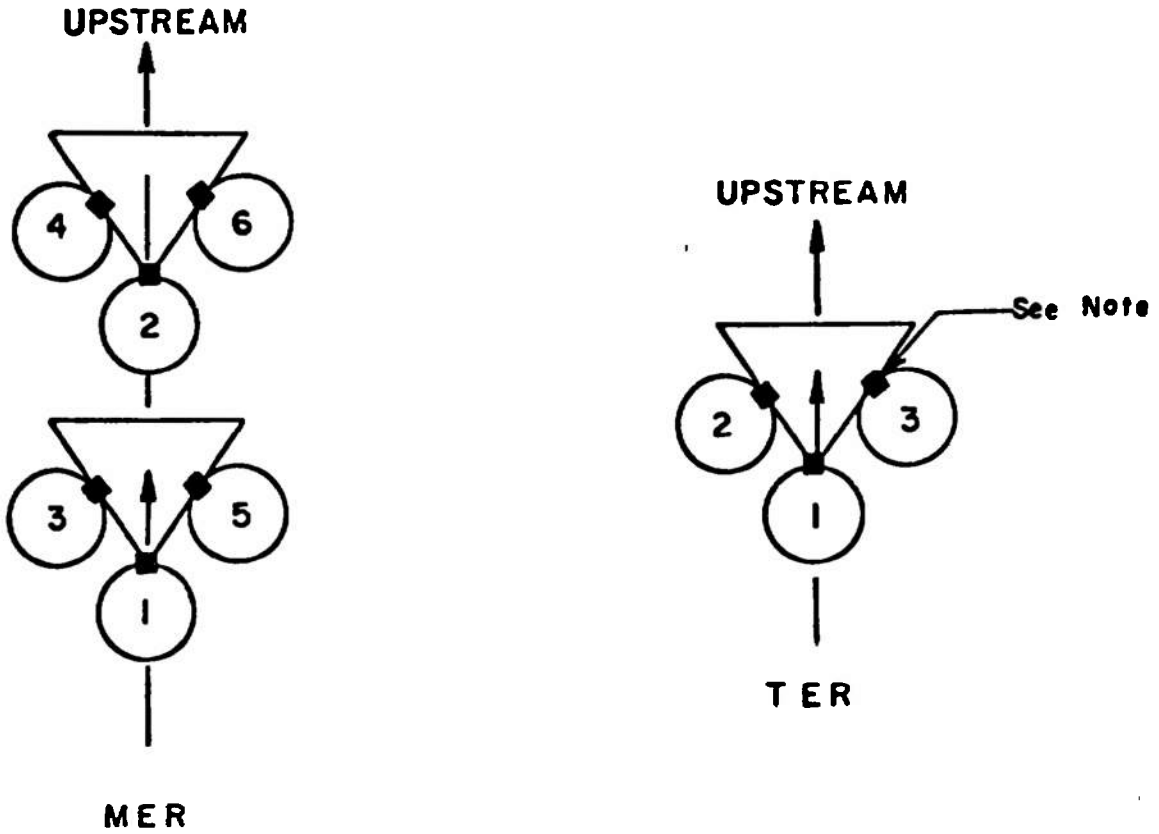

NOTE: The square indicates the orientation of the suspension lugs

TYPE RACK	STATION	ROLL ORIENTATION, deg
MER	1	0
	2	0
	3	45
	4	45
	5	-45
	6	-45
TER	1	0
	2	45
	3	-45

Fig. 19 Identification of the TER and MER Store Stations and Orientations

SYMBOL	CONF	M_∞	α	H	$\bar{\phi}$	EJECTOR FORCE
○	1L	0.33	12.9	4000	0	I
□	1L	0.73	3.4	4000	0	I
△	1L	0.95	2.0	7000	-70	I

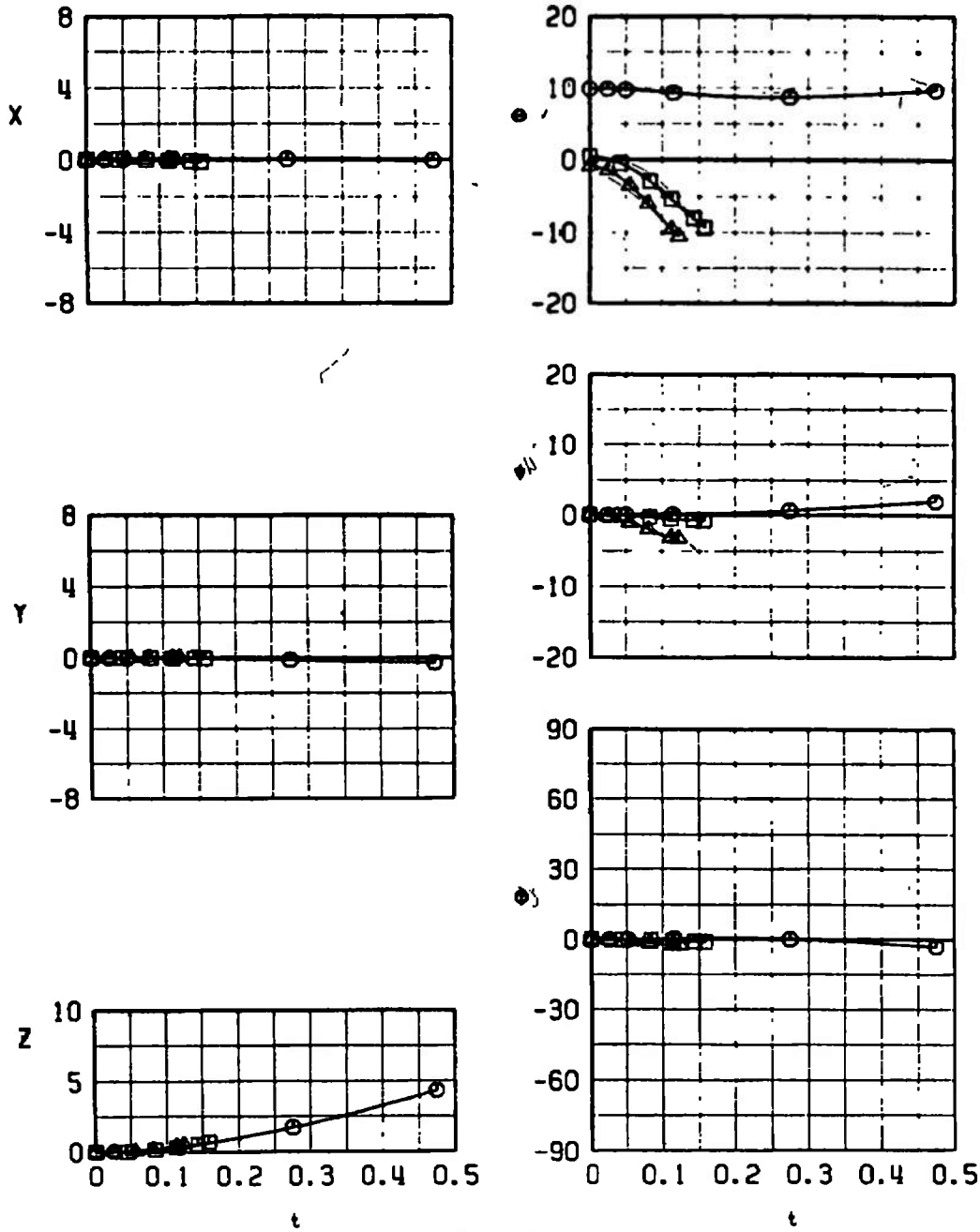

a. Configuration 1L

Fig. 20 Trajectory Data for the MK-84 LGB

SYMBOL	CONF	M_∞	α	H	$\bar{\phi}$	EJECTOR FORCE
○	1R	0.33	12.9	4000	0	I
□	1R	0.73	3.4	4000	0	I
△	1R	0.95	2.0	7000	-70	I

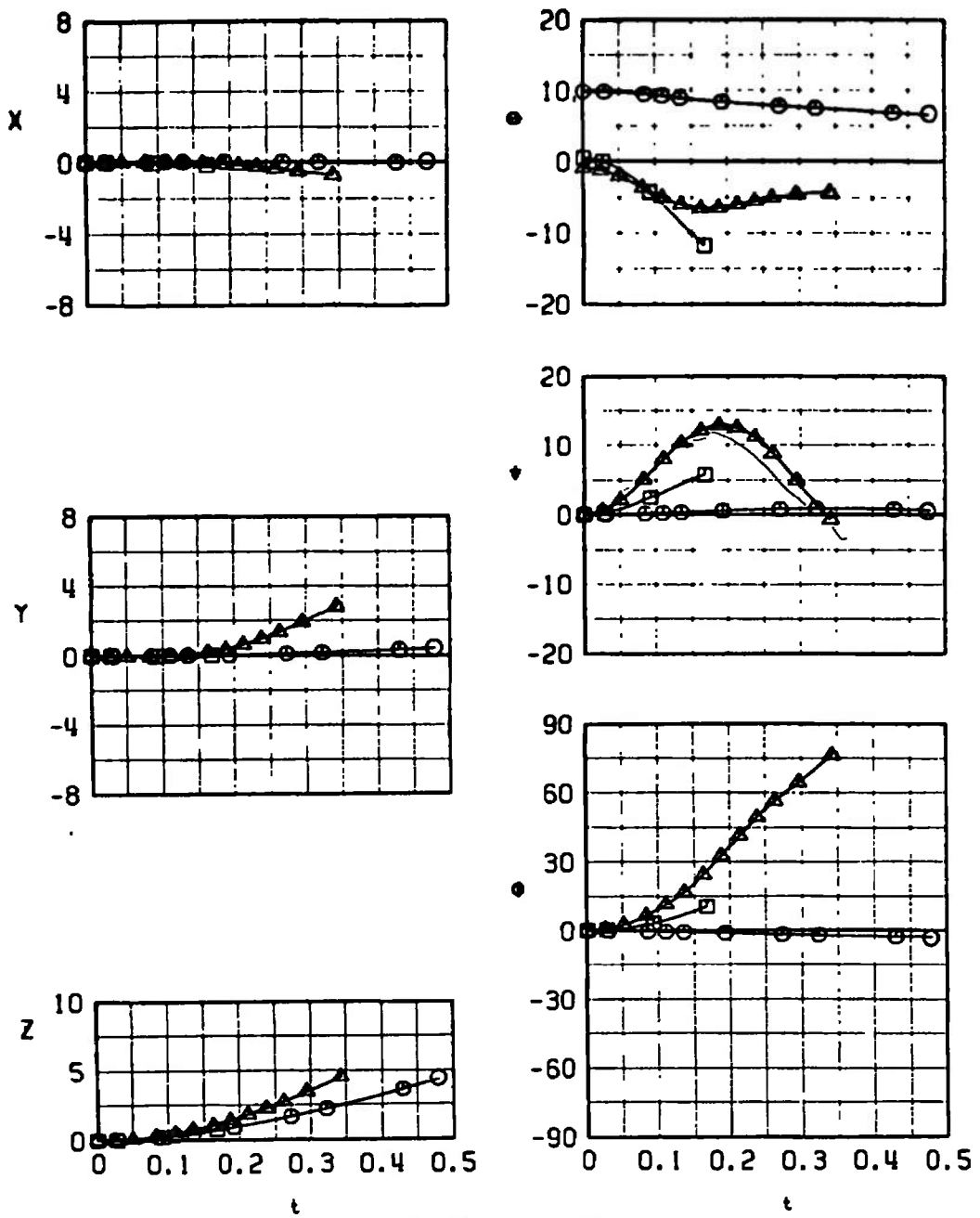

b. Configuration 1R
Fig. 20 Continued

SYMBOL	CONF	M_∞	α	H	$\bar{\phi}$	EJECTOR FORCE
□	2L	0.73	3.4	4000	0	I
△	2L	0.95	2.0	7000	-70	I

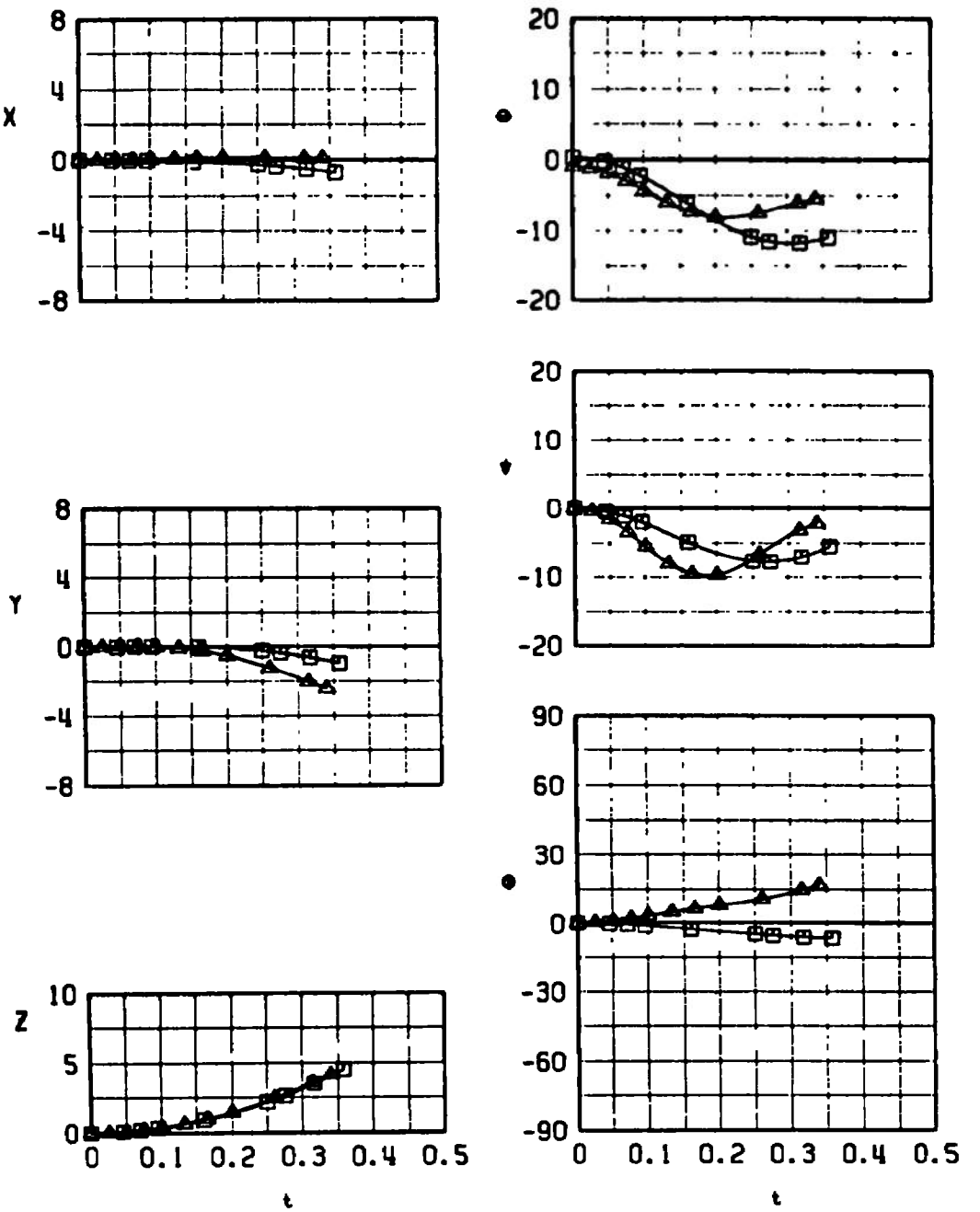

c. Configuration 2L
Fig. 20 Continued

SYMBOL	CONF	M_∞	α	H	$\bar{\phi}$	EJECTOR FORCE
○	2R	0.33	12.9	4000	0	I
□	2R	0.73	3.4	4000	0	I
△	2R	0.95	2.0	7000	-70	I

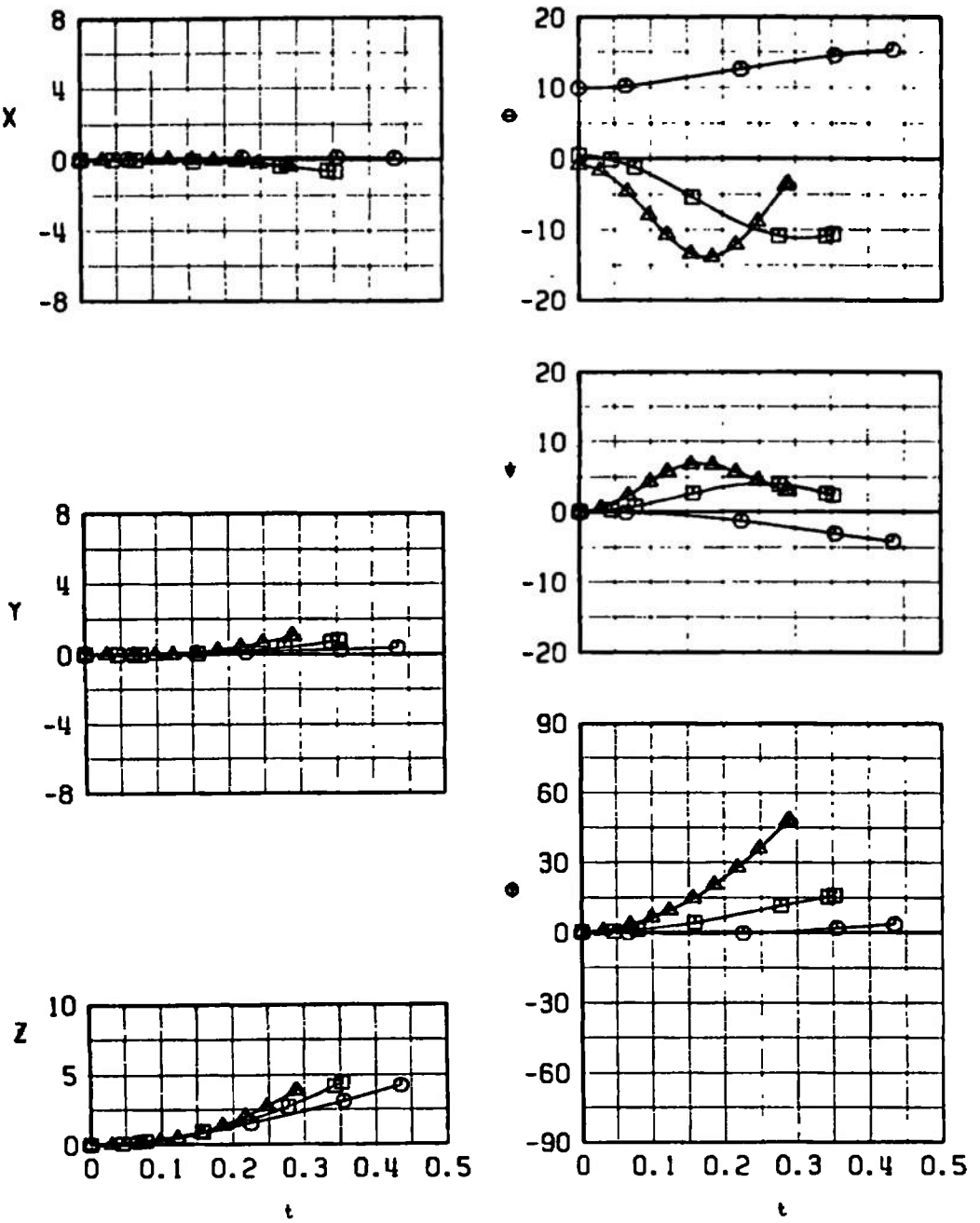

d. Configuration 2R
Fig. 20 Concluded

SYMBOL	CONF	M_∞	α	H	$\bar{\phi}$	EJECTOR FORCE
○	3L	0.33	12.9	4000	0	2
□	3L	0.73	3.4	4000	0	2
△	3L	0.95	2.0	7000	-70	2

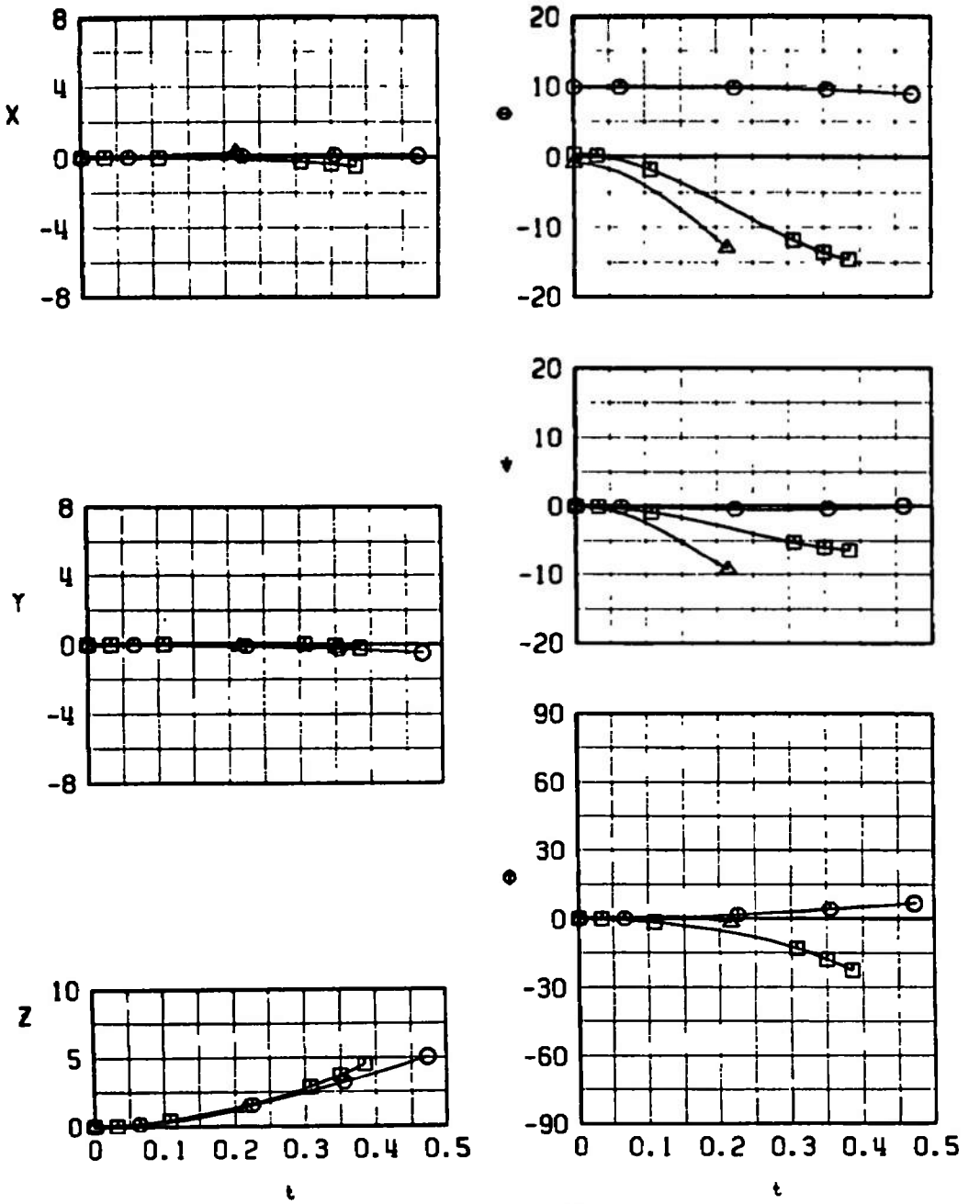

a. Configuration 3L

Fig. 21 Trajectory Data for the MK-84 EOGB

SYMBOL	CONF	M_∞	α	H	$\bar{\phi}$	EJECTOR FORCE
○	3R	0.33	12.9	4000	0	2
□	3R	0.73	3.4	4000	0	2
△	3R	0.95	2.0	7000	-70	2

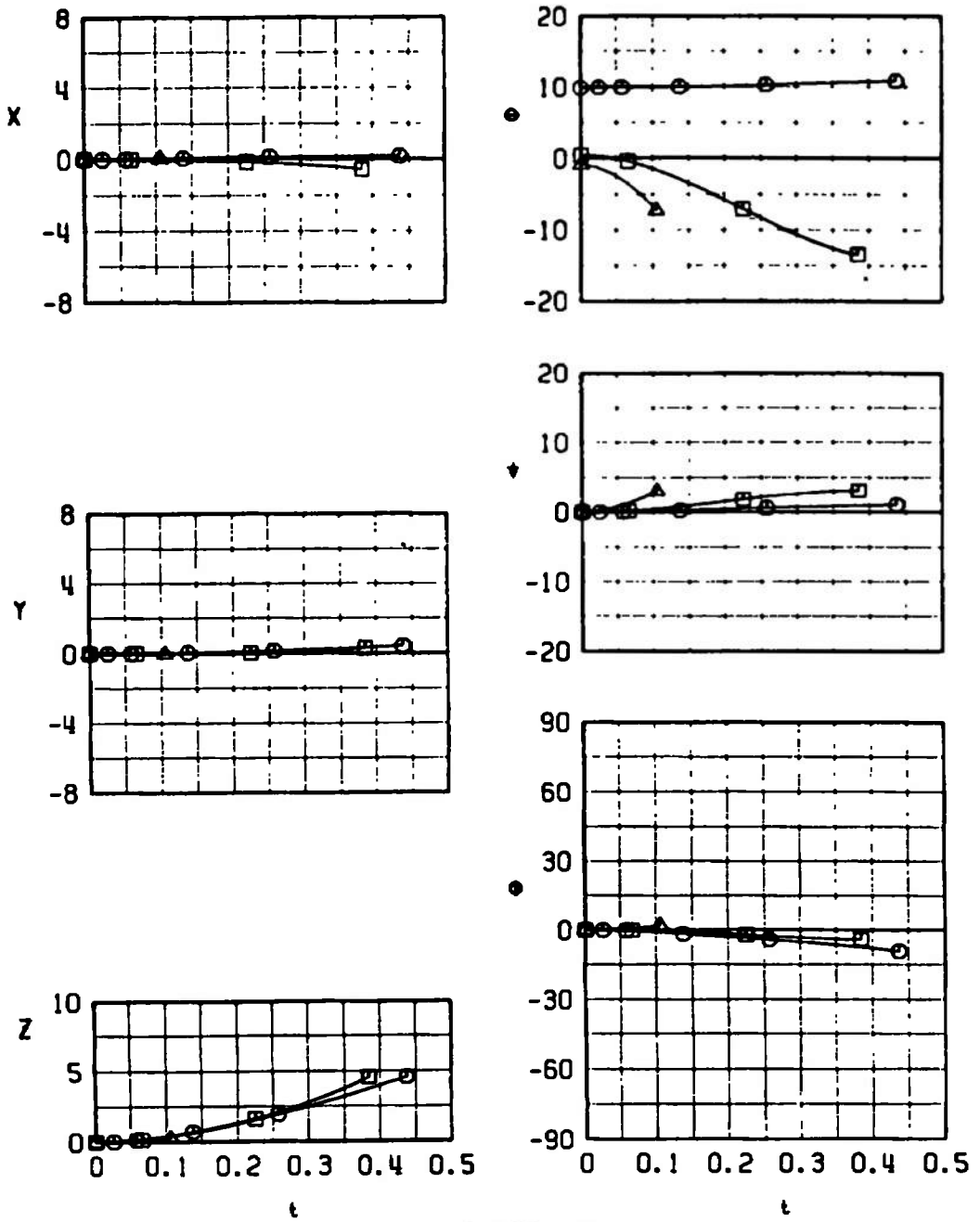

b. Configuration 3R
Fig. 21 Continued

SYMBOL	CONF	M_∞	α	H	$\bar{\phi}$	EJECTOR FORCE
○	4L	0.33	12.9	4000	0	2
□	4L	0.73	3.4	4000	0	2
△	4L	0.95	2.0	7000	-70	2

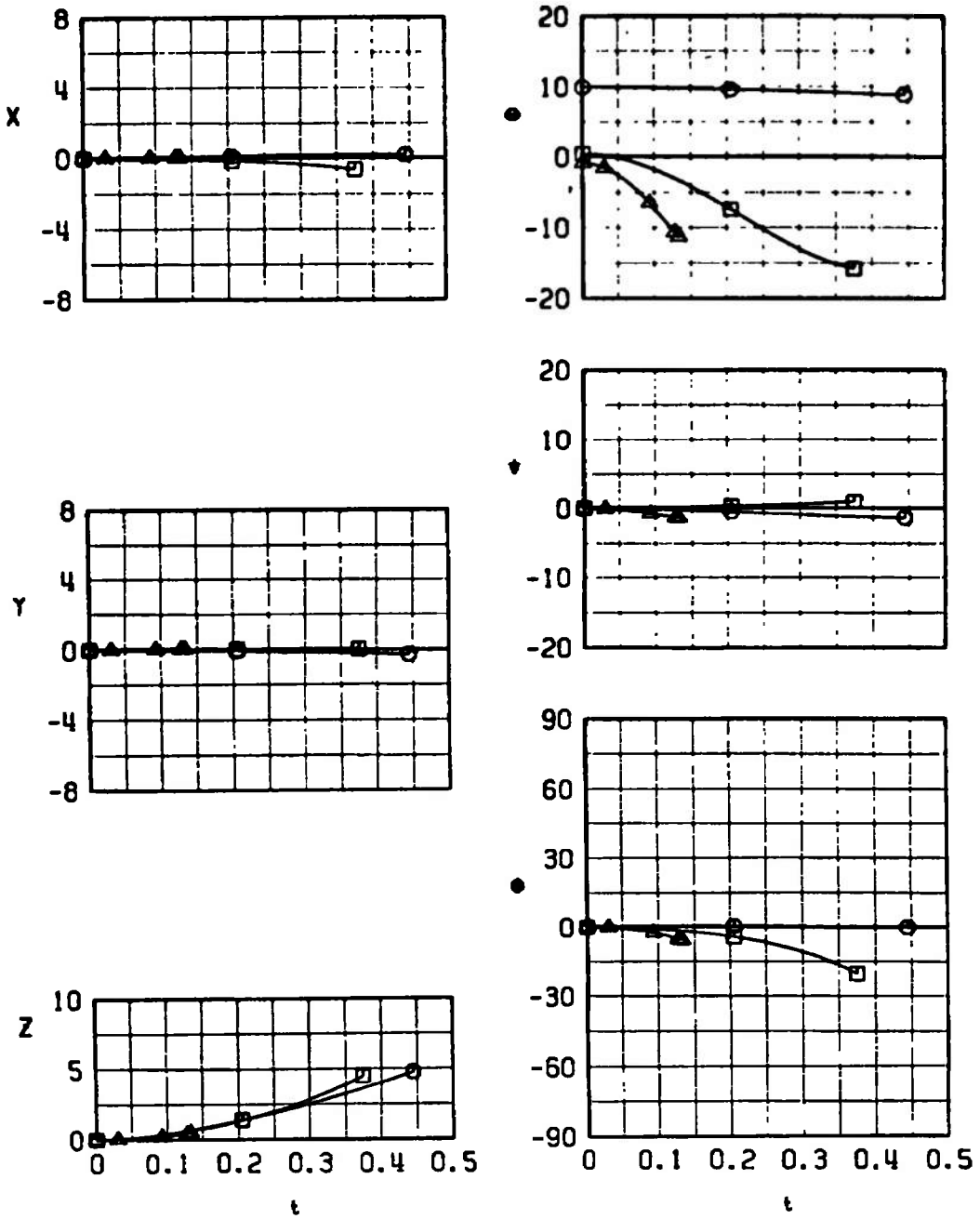

c. Configuration 4L
Fig. 21 Continued

SYMBOL	CONF	M_∞	α	H	$\bar{\phi}$	EJECTOR FORCE
○	4R	0.33	12.9	4000	0	2
□	4R	0.73	3.4	4000	0	2
△	4R	0.95	2.0	7000	-70	2

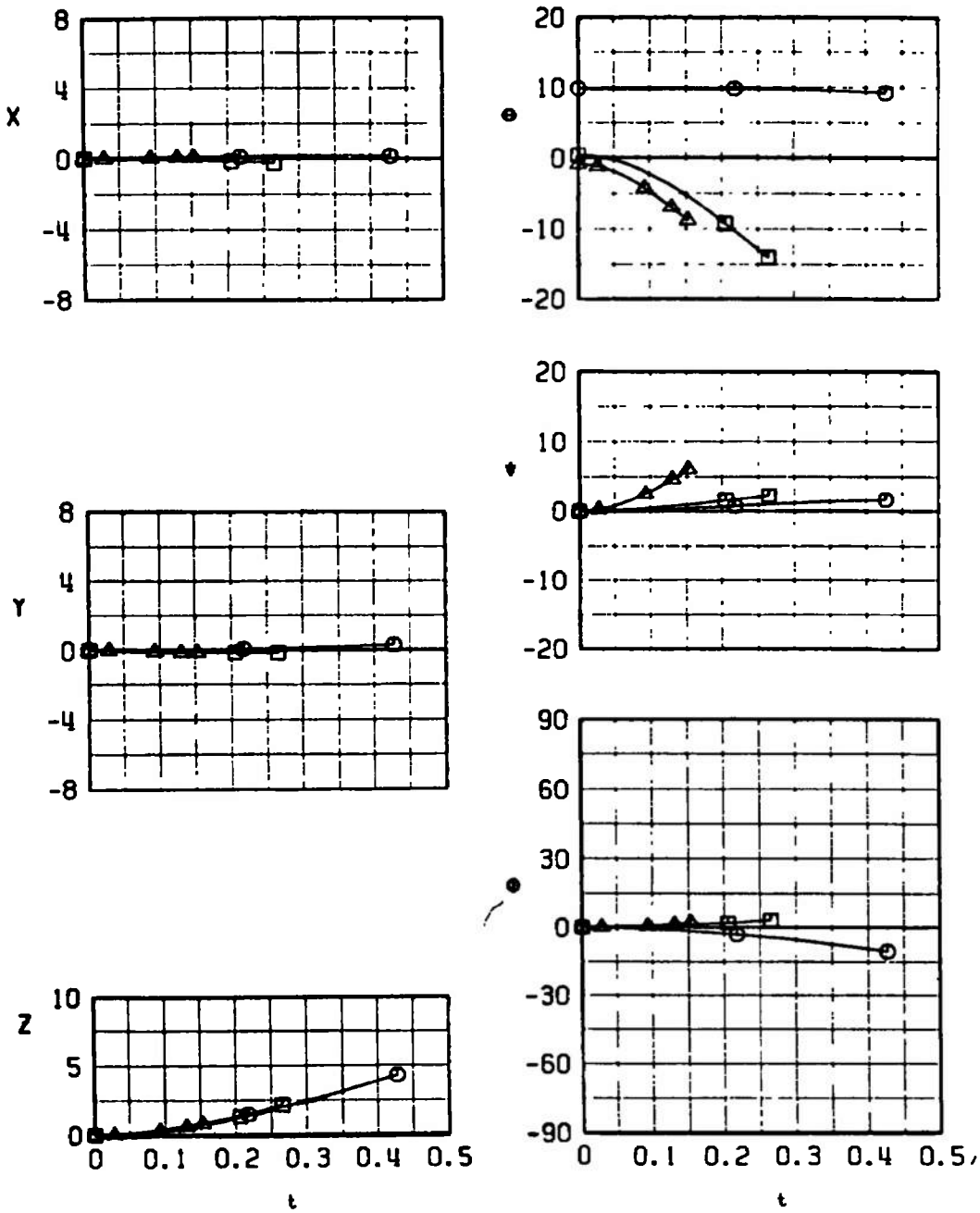

d. Configuration 4R
Fig. 21 Concluded

SYMBOL	CONF	M_∞	α	H	$\bar{\theta}$	EJECTOR FORCE
⊙	5L	0.33	12.9	4000	0	3
⊡	5L	0.73	3.4	4000	0	3
△	5L	0.95	2.0	7000	-70	3

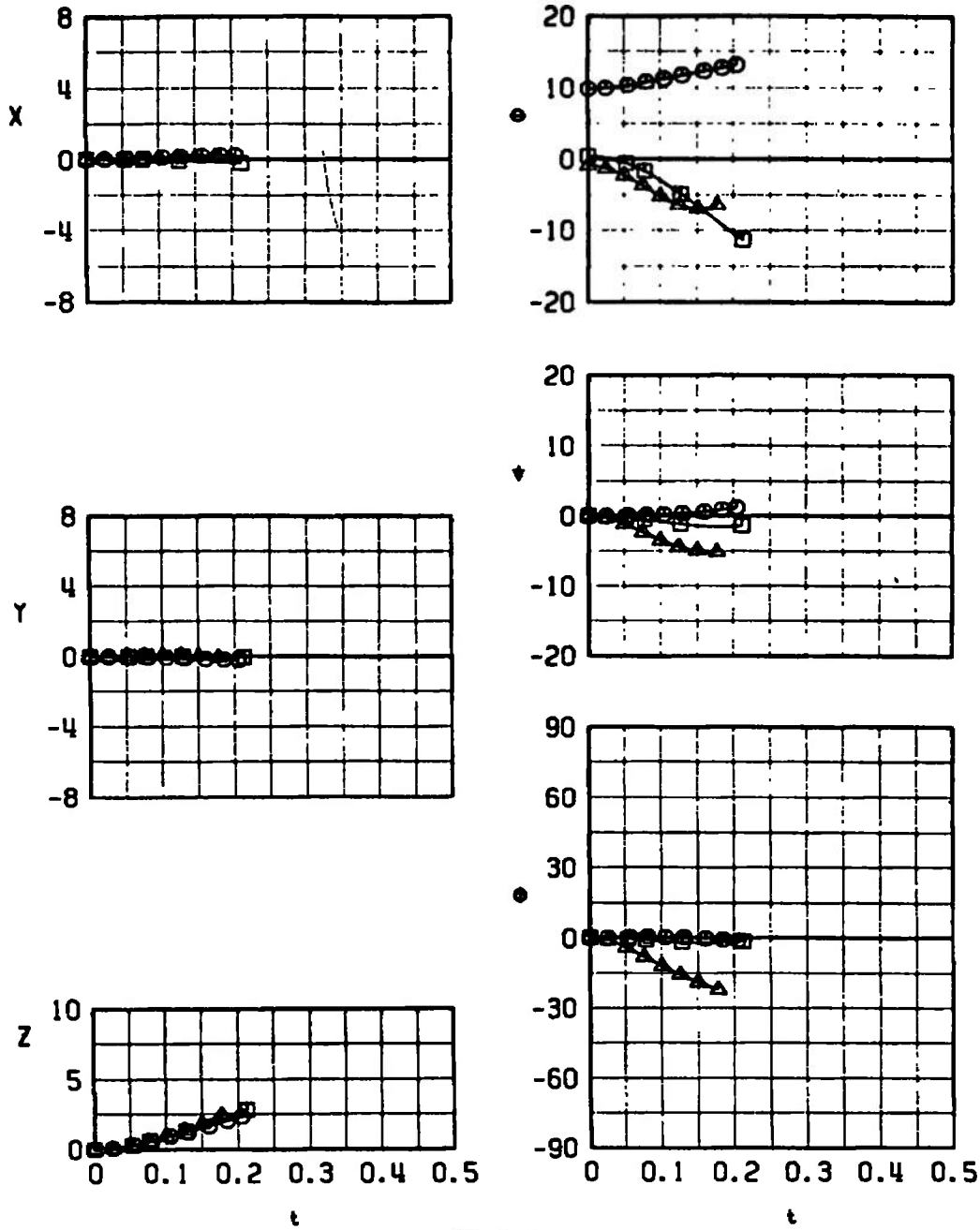

a. Configuration 5L

Fig. 22 Trajectory Data for the MK-82 LGB

SYMBOL	CONF	M_∞	α	H	$\bar{\phi}$	EJECTOR FORCE
○	5R	0.33	12.9	4000	0	3
□	5R	0.73	3.4	4000	0	3
△	5R	0.95	2.0	7000	-70	3

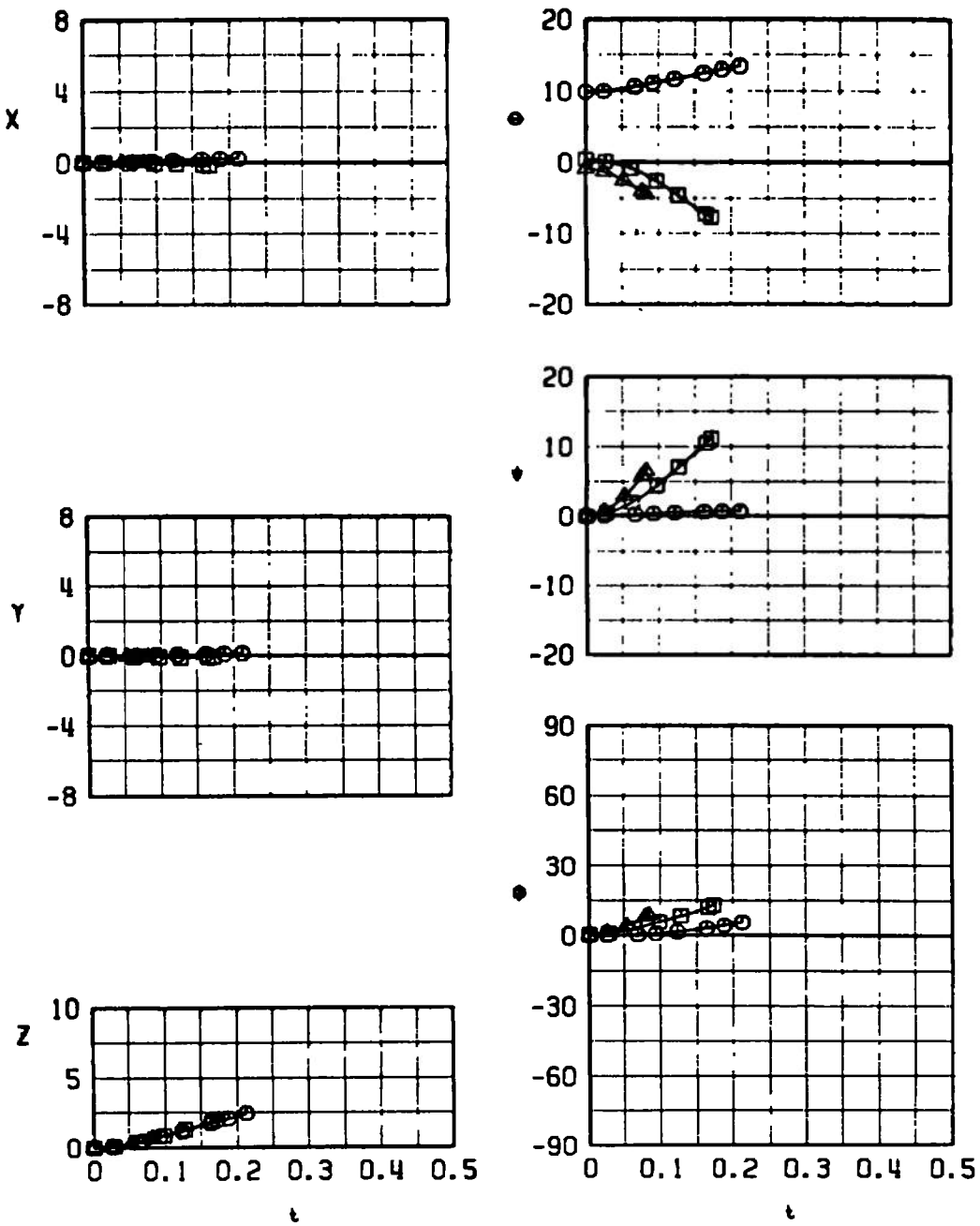

b. Configuration 5R
Fig. 22 Continued

SYMBOL	CONF	M_∞	α	H	$\bar{\phi}$	EJECTOR FORCE
○	6L	0.33	12.9	4000	0	3
□	6L	0.73	3.4	4000	0	3
△	6L	0.95	2.0	7000	-70	3

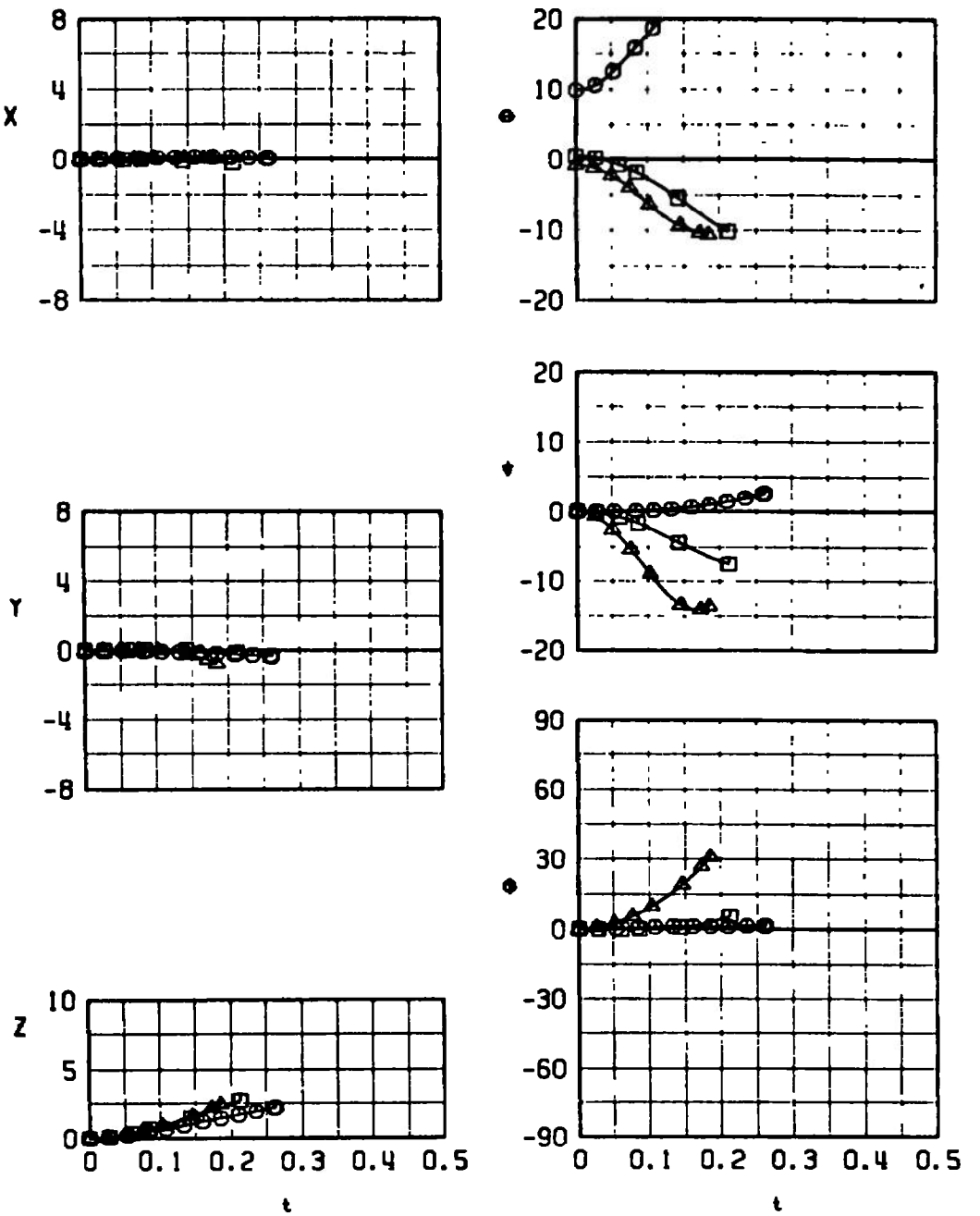

c. Configuration 6L
Fig. 22 Continued

SYMBOL	CONF	M_∞	α	H	$\bar{\phi}$	EJECTOR FORCE
○	6R	0.33	12.9	4000	0	3
□	6R	0.73	3.4	4000	0	3
△	6R	0.95	2.0	7000	-70	3

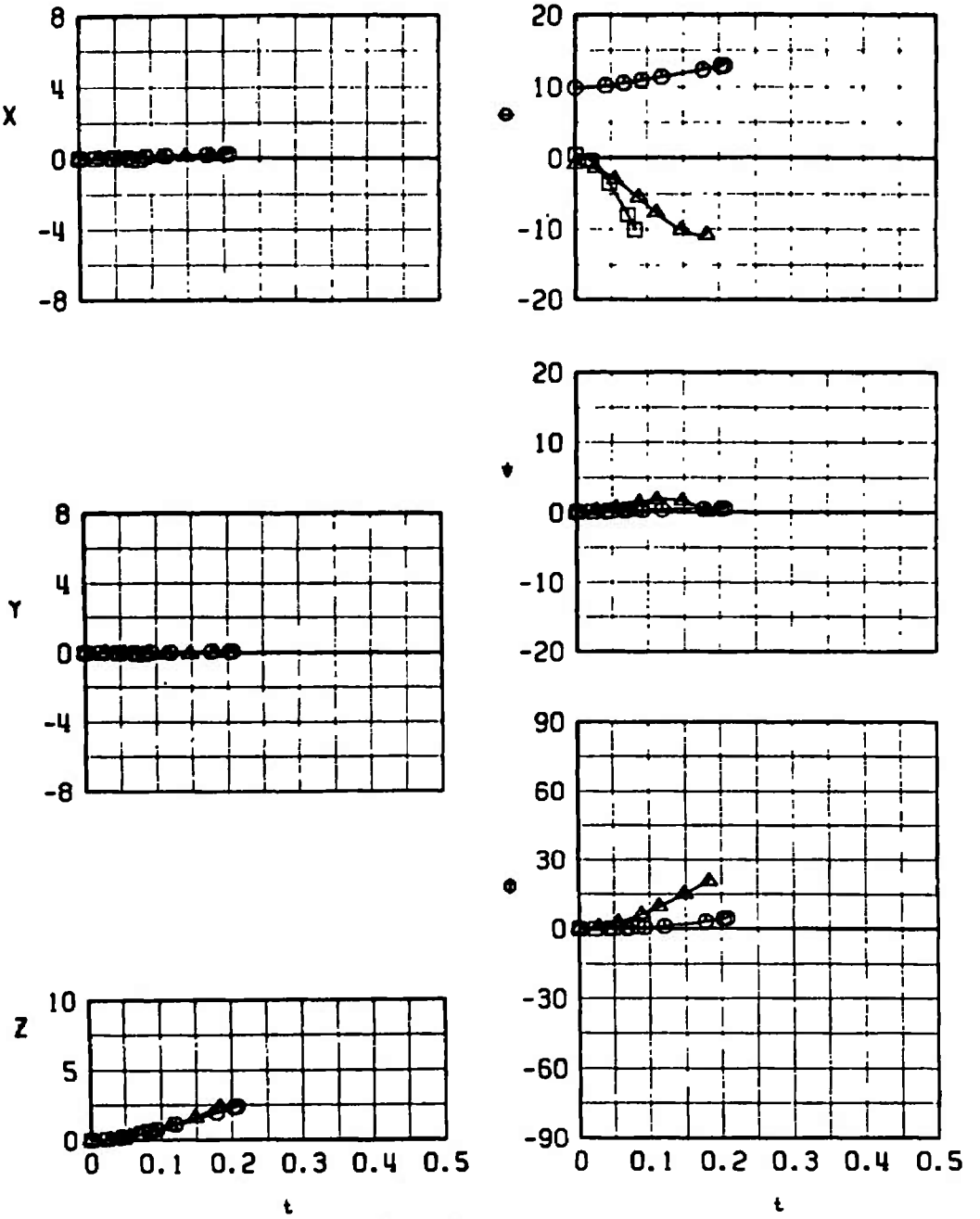

d. Configuration 6R
Fig. 22 Continued

SYMBOL	CONF	M_∞	α	H	$\bar{\phi}$	EJECTOR FORCE
⊙	7L	0.90	2.1	9000	-70	3

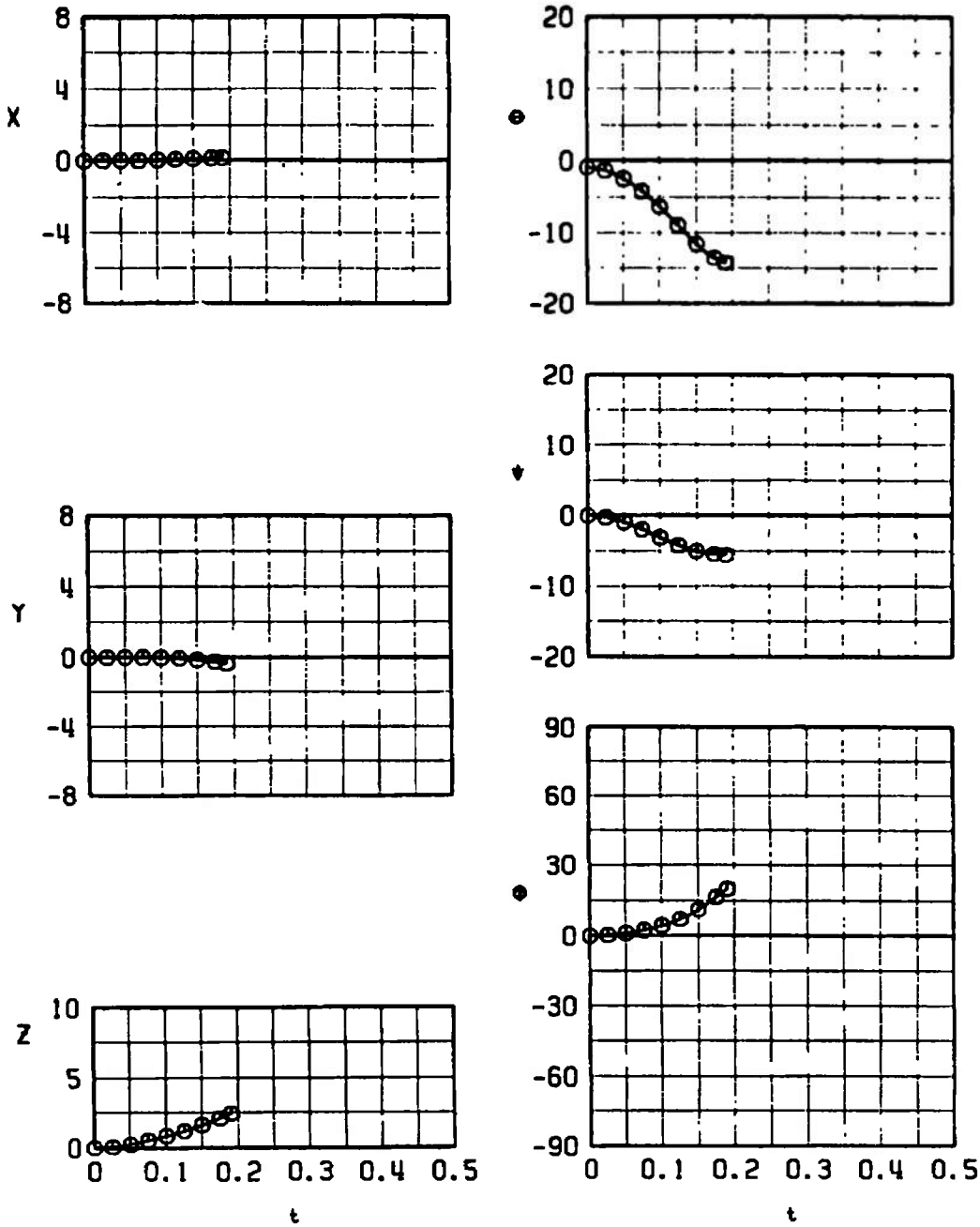

e. Configuration 7L
Fig. 22 Continued

SYMBOL	CONF	M_∞	α	H	$\bar{\phi}$	EJECTOR FORCE
⊙	7R	0.95	2.0	7000	-70	3

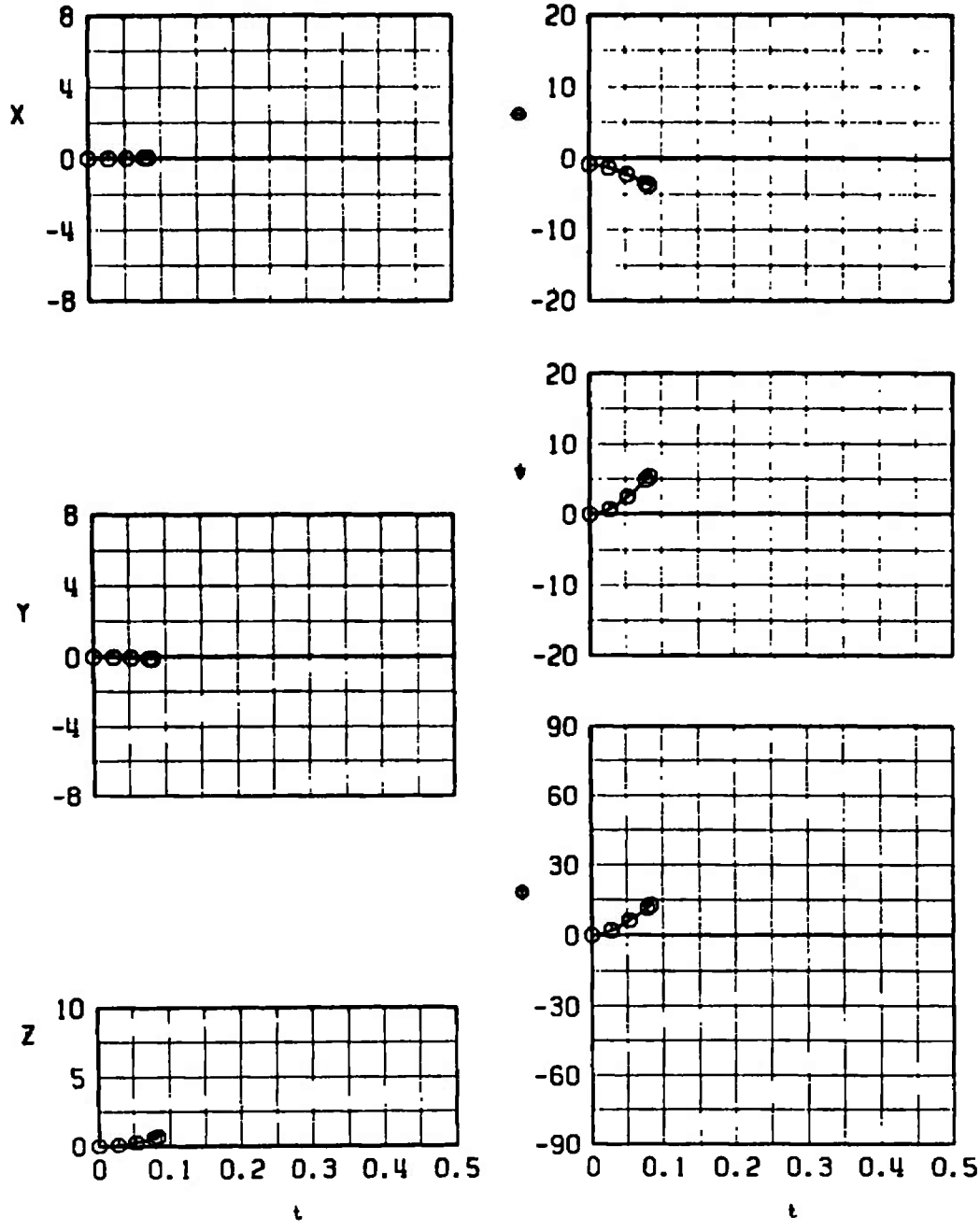

f. Configuration 7R
Fig. 22 Continued

SYMBOL	CONF	M_∞	α	H	$\bar{\phi}$	EJECTOR FORCE
○	8L	0.33	12.9	4000	0	4
□	8L	0.73	3.4	4000	0	4
△	8L	0.95	2.0	7000	-70	4

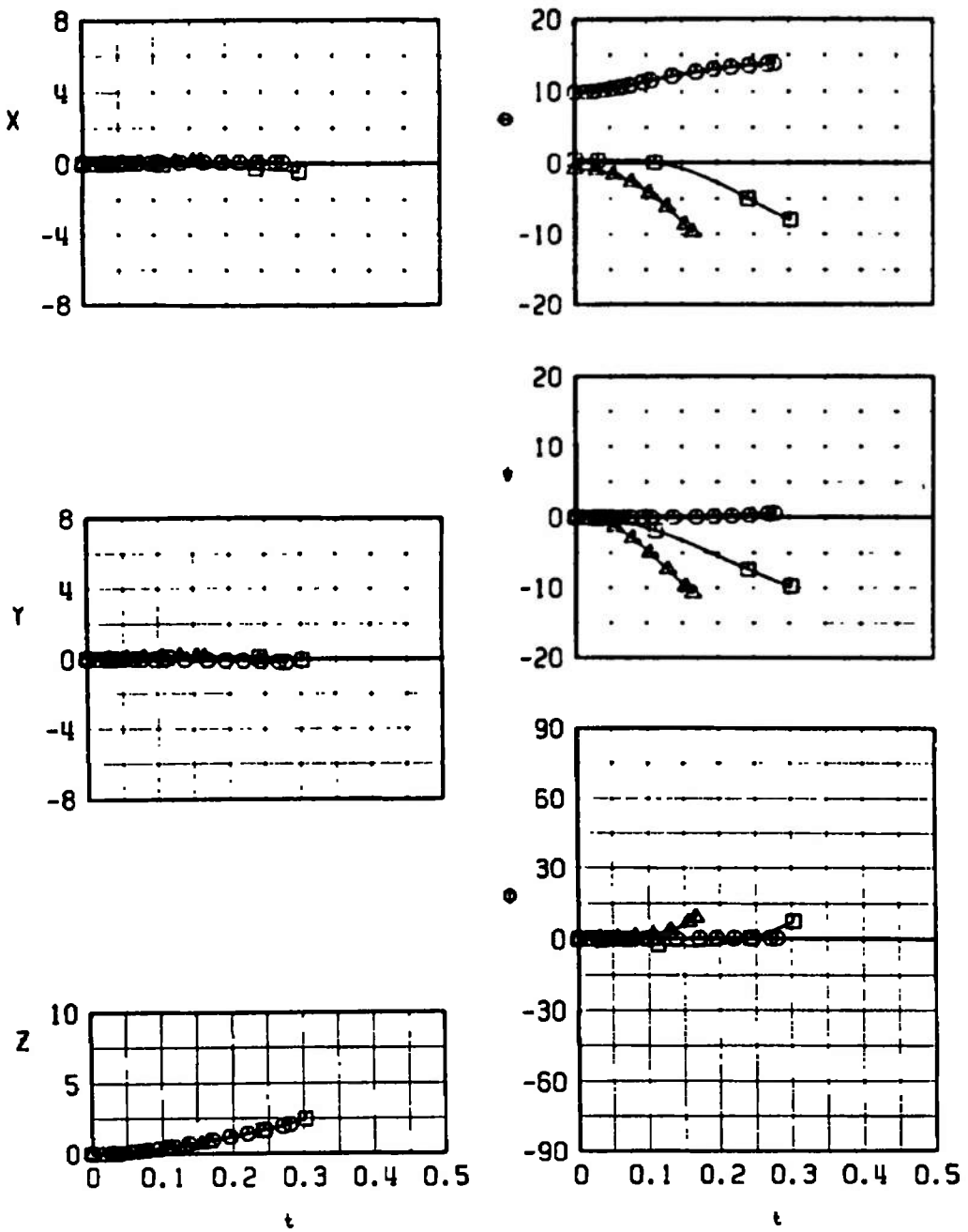

g. Configuration 8L
Fig. 22 Continued

SYMBOL	CONF	M_∞	α	H	$\bar{\Theta}$	EJECTOR FORCE
○	8R	0.33	12.9	4000	0	4
□	8R	0.73	3.4	4000	0	4
△	8R	0.95	2.0	7000	-70	4

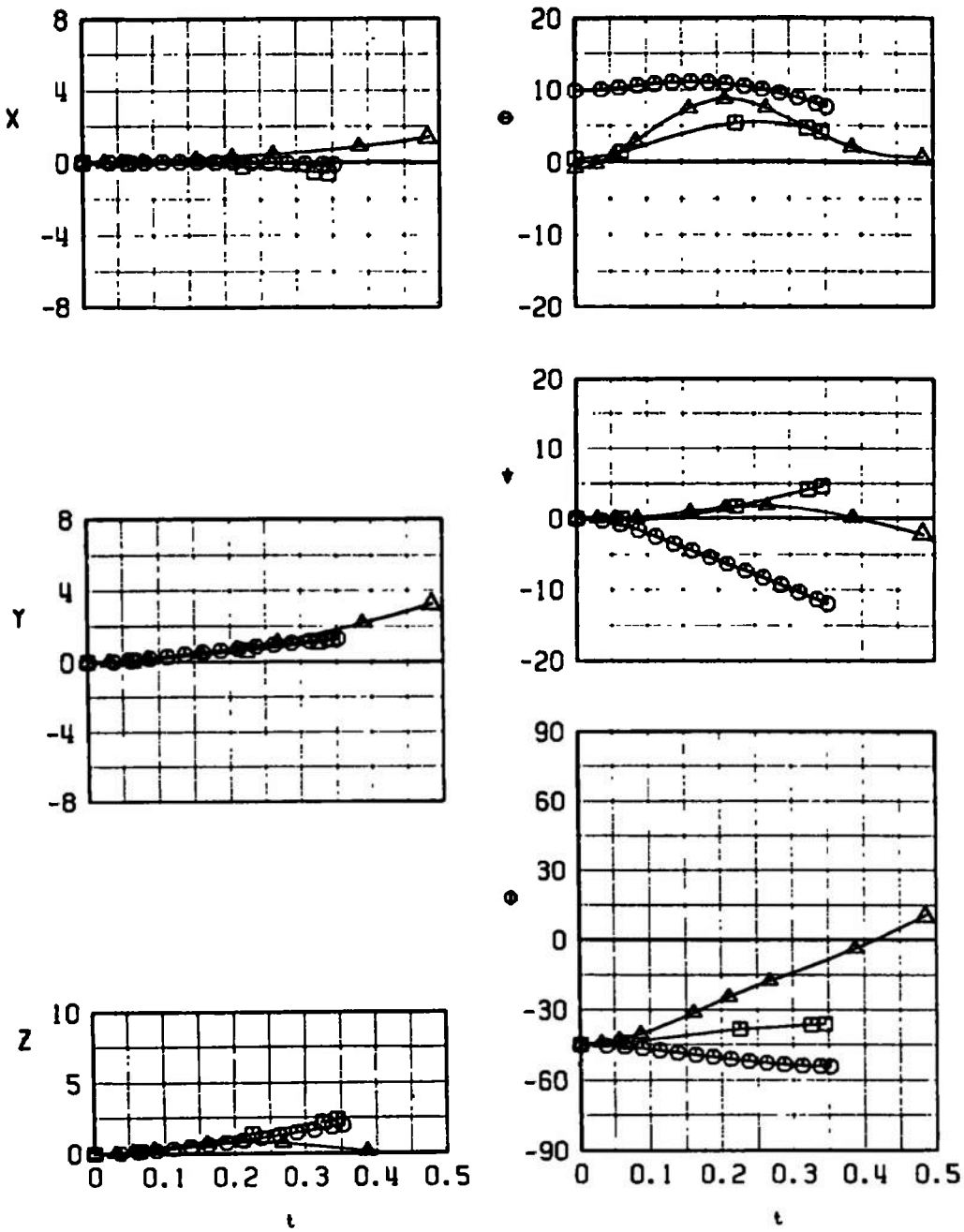

h. Configuration 8R
Fig. 22 Continued

SYMBOL	CONF	M_∞	α	H	$\bar{\phi}$	EJECTOR FORCE
○	9L	0.33	12.9	4000	0	4
□	9L	0.73	3.4	4000	0	4
△	9L	0.95	2.0	7000	-70	4

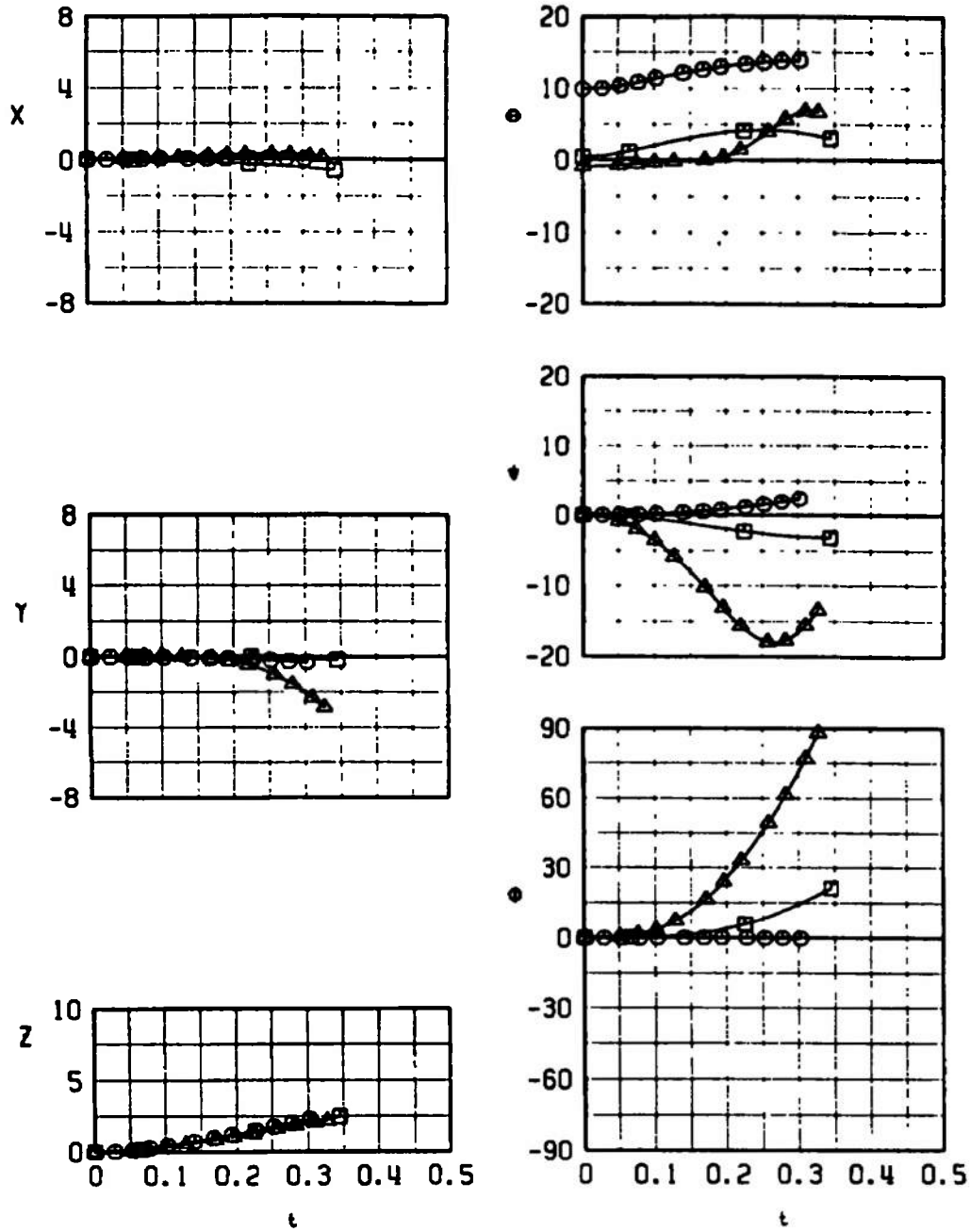

i. Configuration 9L
Fig. 22 Continued

SYMBOL	CONF	M_∞	α	H	$\bar{\phi}$	EJECTOR FORCE
○	9R	0.33	12.9	4000	0	4
□	9R	0.73	3.4	4000	0	4
△	9R	0.95	2.0	7000	-70	4

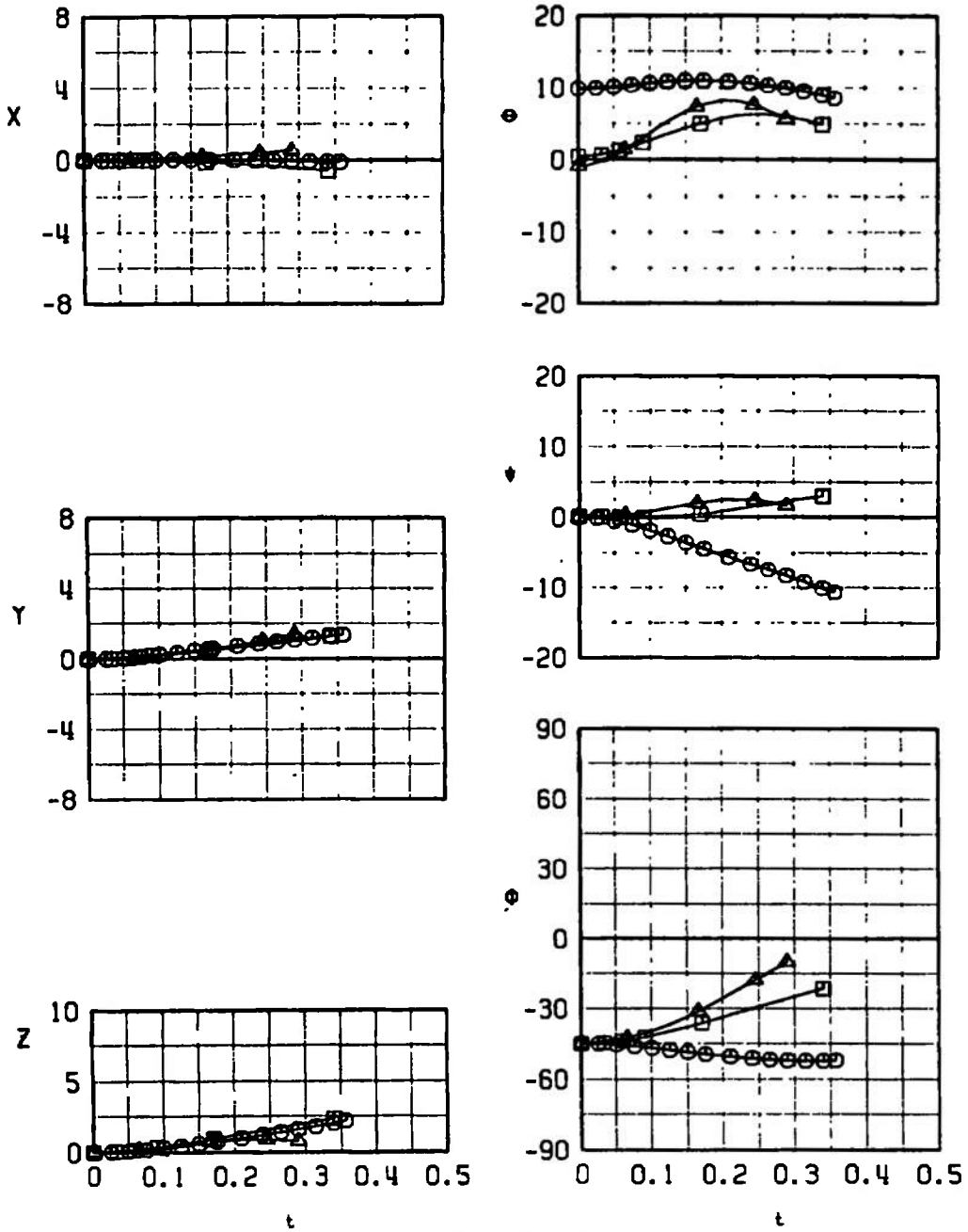

j. Configuration 9R
Fig. 22 Concluded

SYMBOL	CONF	M_∞	α	H	$\bar{\sigma}$	EJECTOR FORCE
⊙	10L	0.41	8.6	4000	0	6
⊡	10L	0.73	3.4	4000	0	6
△	10L	0.90	3.4	15000	0	6

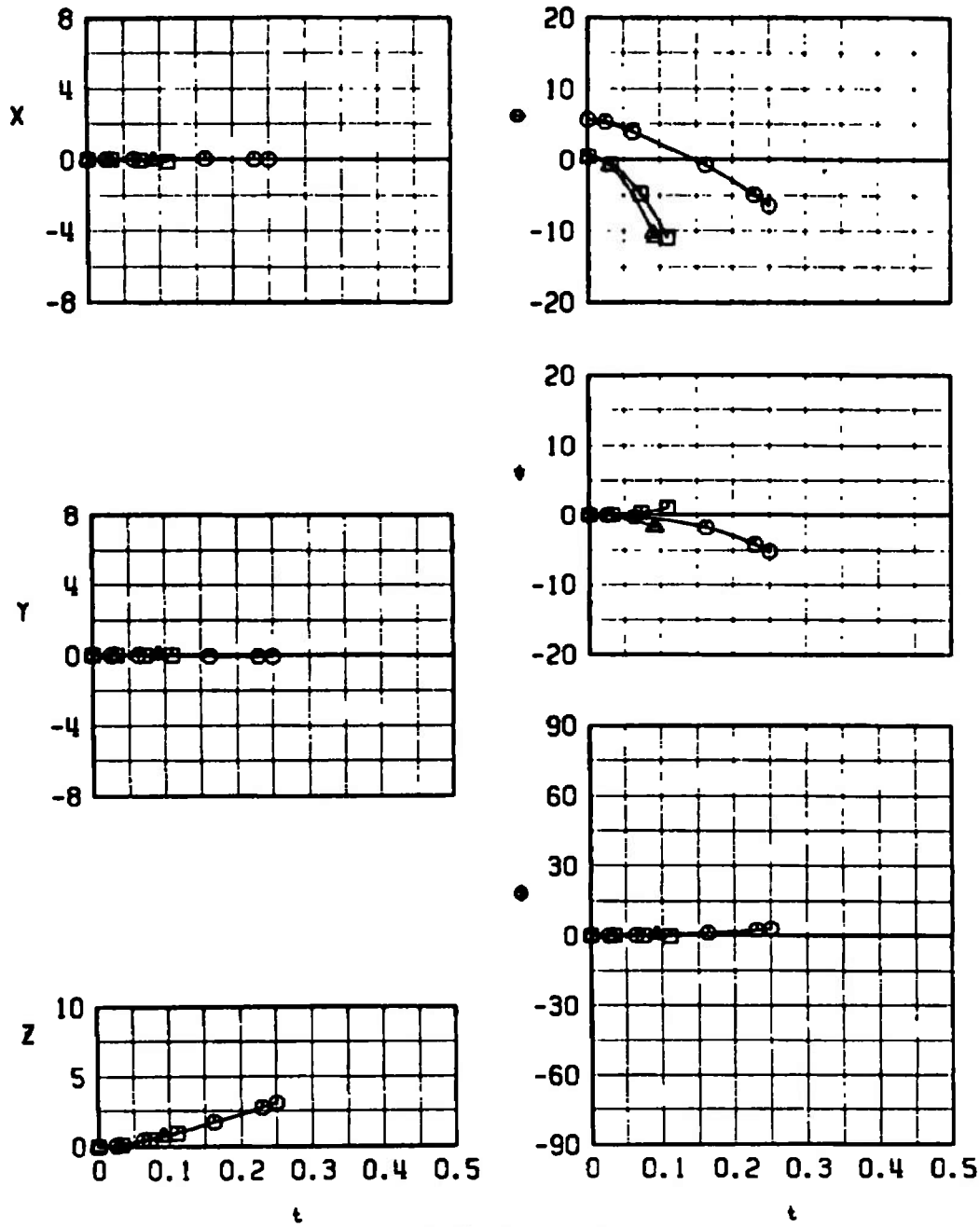

a. Configuration 10L

Fig. 23 Trajectory Data for the Loaded LAU-68 A/A

SYMBOL	CONF	M_∞	α	H	$\bar{\bullet}$	EJECTOR FORCE
○	10R	0.41	8.6	4000	0	6
□	10R	0.73	4.9	4000	0	6
△	10R	0.90	3.4	15000	0	6

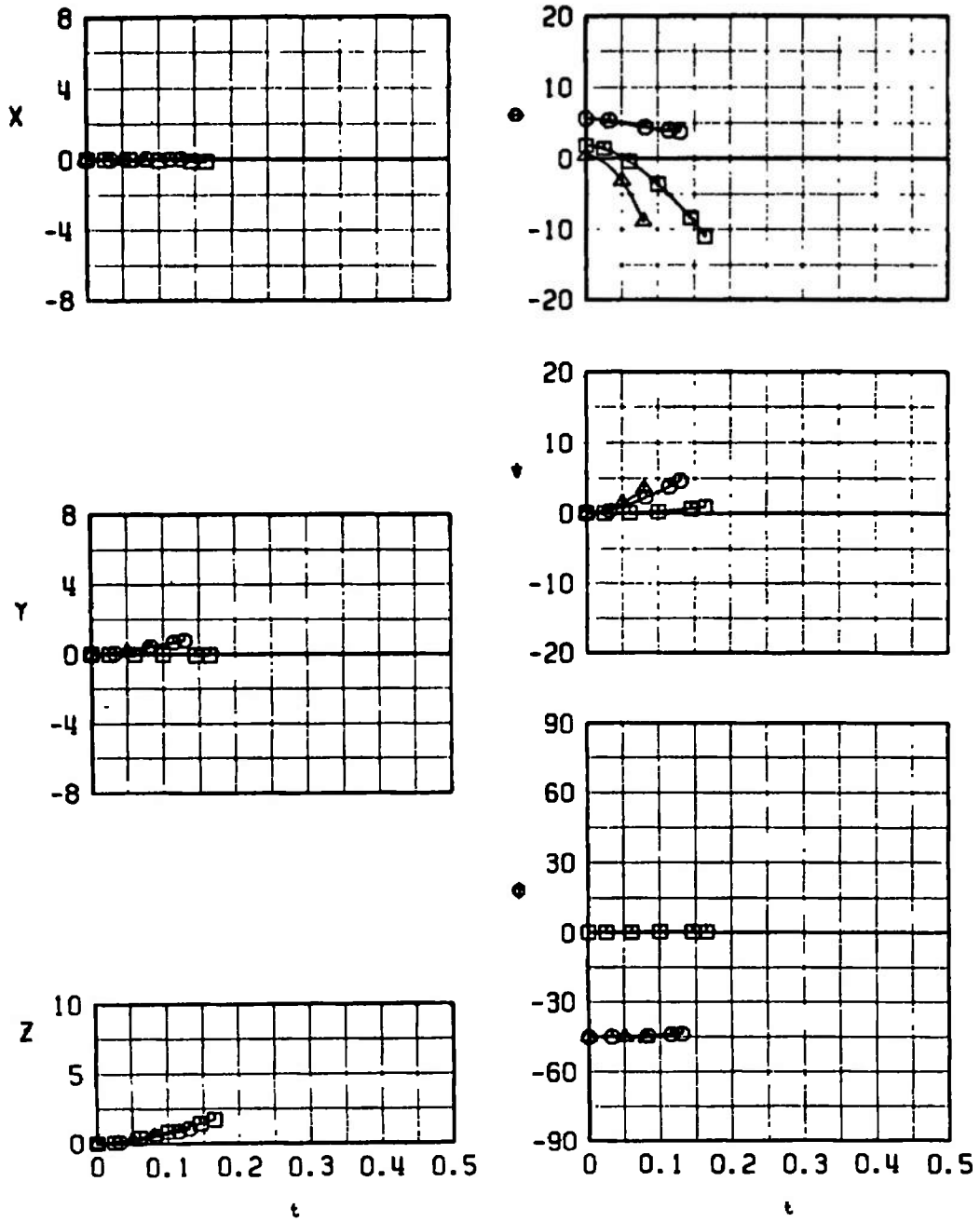

b. Configuration 10R
Fig. 23 Concluded

SYMBOL	CONF	M_∞	α	H	$\bar{\phi}$	EJECTOR FORCE
○	11L	0.41	8.6	4000	0	5
□	11L	0.73	3.4	4000	0	5
△	11L	0.90	3.4	15000	0	5

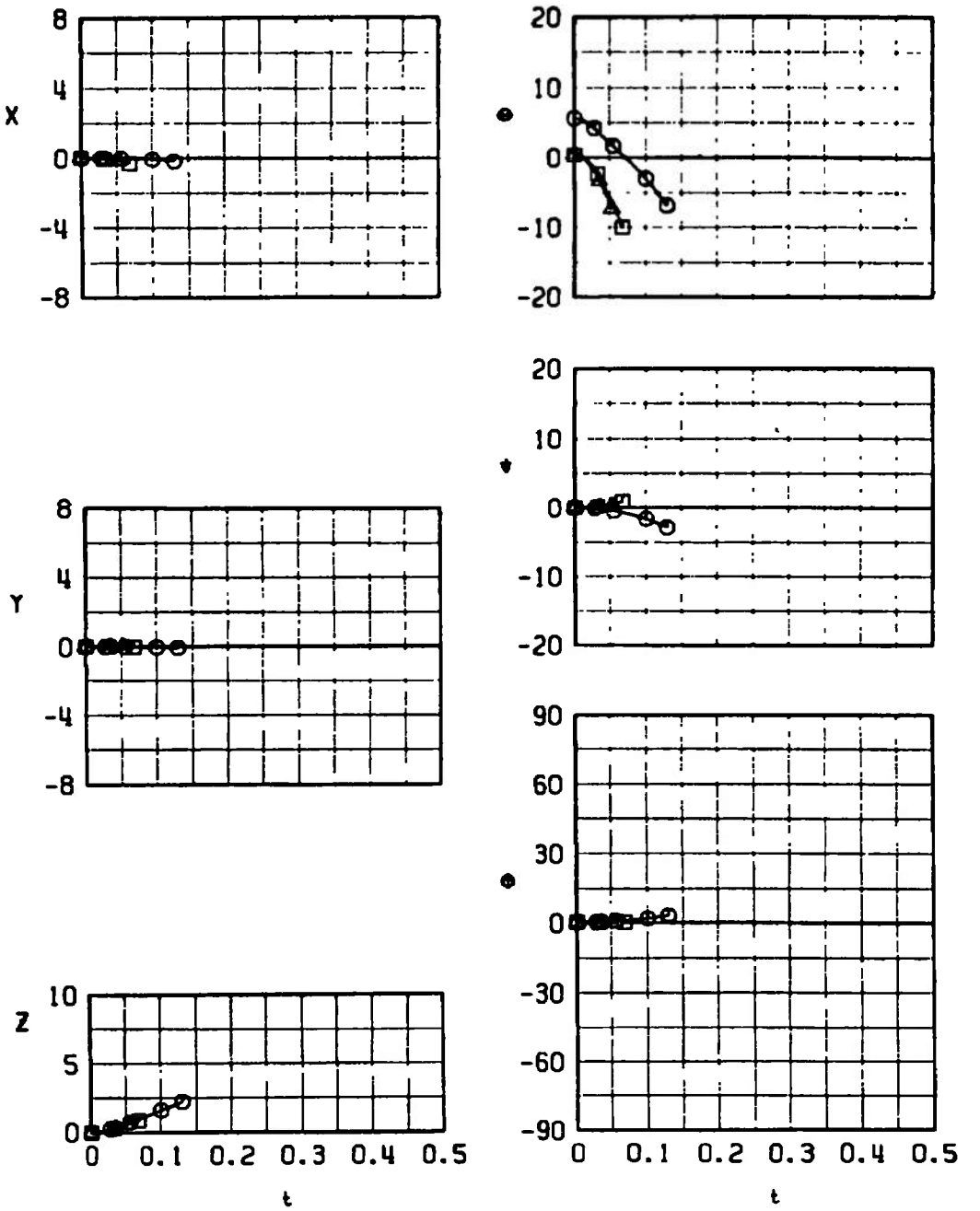

a. Configuration 11L

Fig. 24 Trajectory Data for the Expended LAU-68 A/A

SYMBOL	CONF	M_∞	α	H	$\bar{\delta}$	EJECTOR FORCE
○	11R	0.41	8.6	4000	0	5
□	11R	0.73	3.4	4000	0	5
△	11R	0.90	3.4	15000	0	5

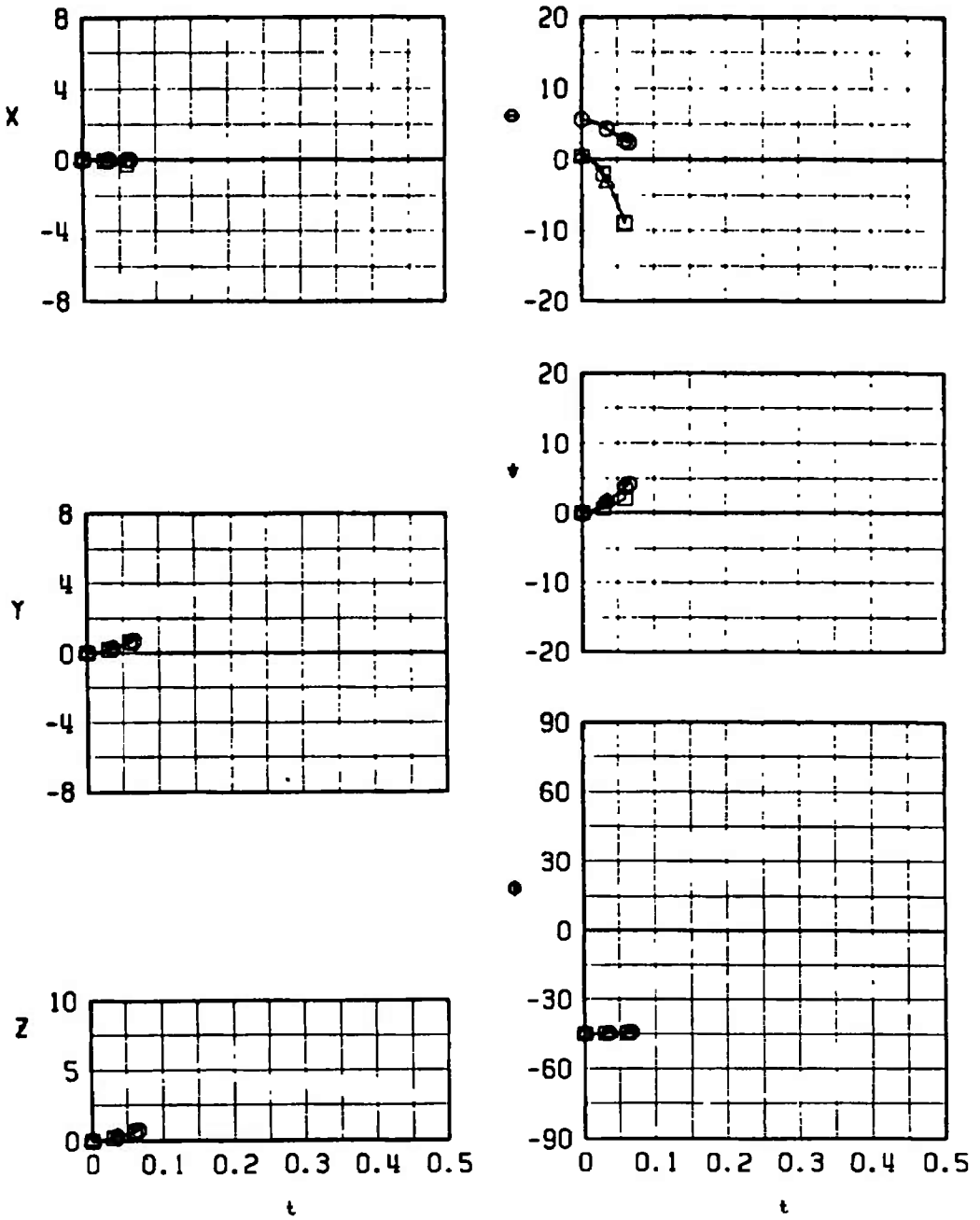

b. Configuration 11R
Fig. 24 Concluded

SYMBOL	CONF	M_∞	α	H	$\bar{\theta}$	EJECTOR FORCE
○	12L	0.80	3.0	15000	-50	7
□	12L	0.90	2.4	15000	-50	7

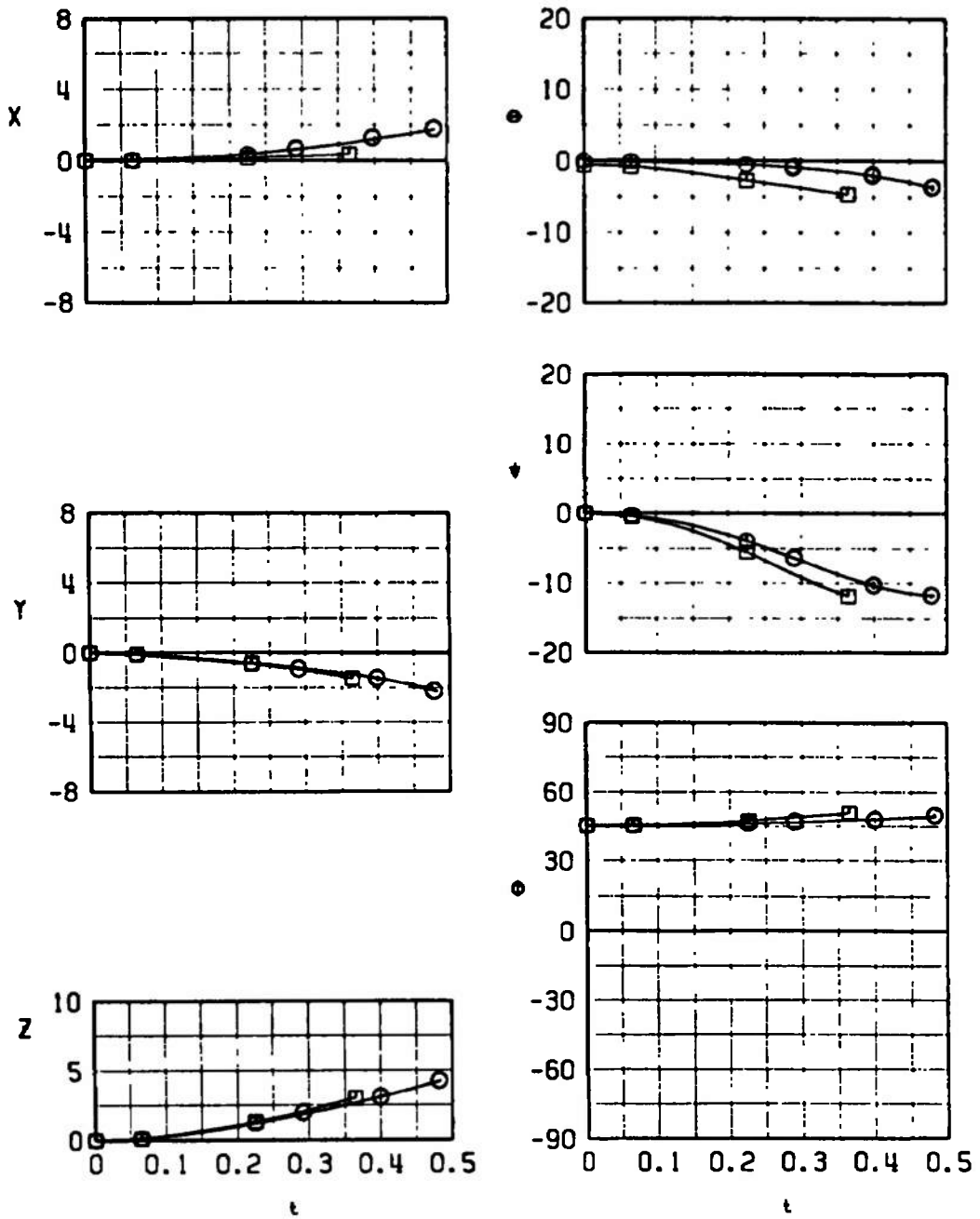

a. Configuration 12L

Fig. 25 Trajectory Data for the BLU 1/B

SYMBOL	CONF	M_∞	α	H	$\bar{\phi}$	EJECTOR FORCE
○	12R	0.80	3.0	15000	0	7
□	12R	0.90	2.4	15000	0	7

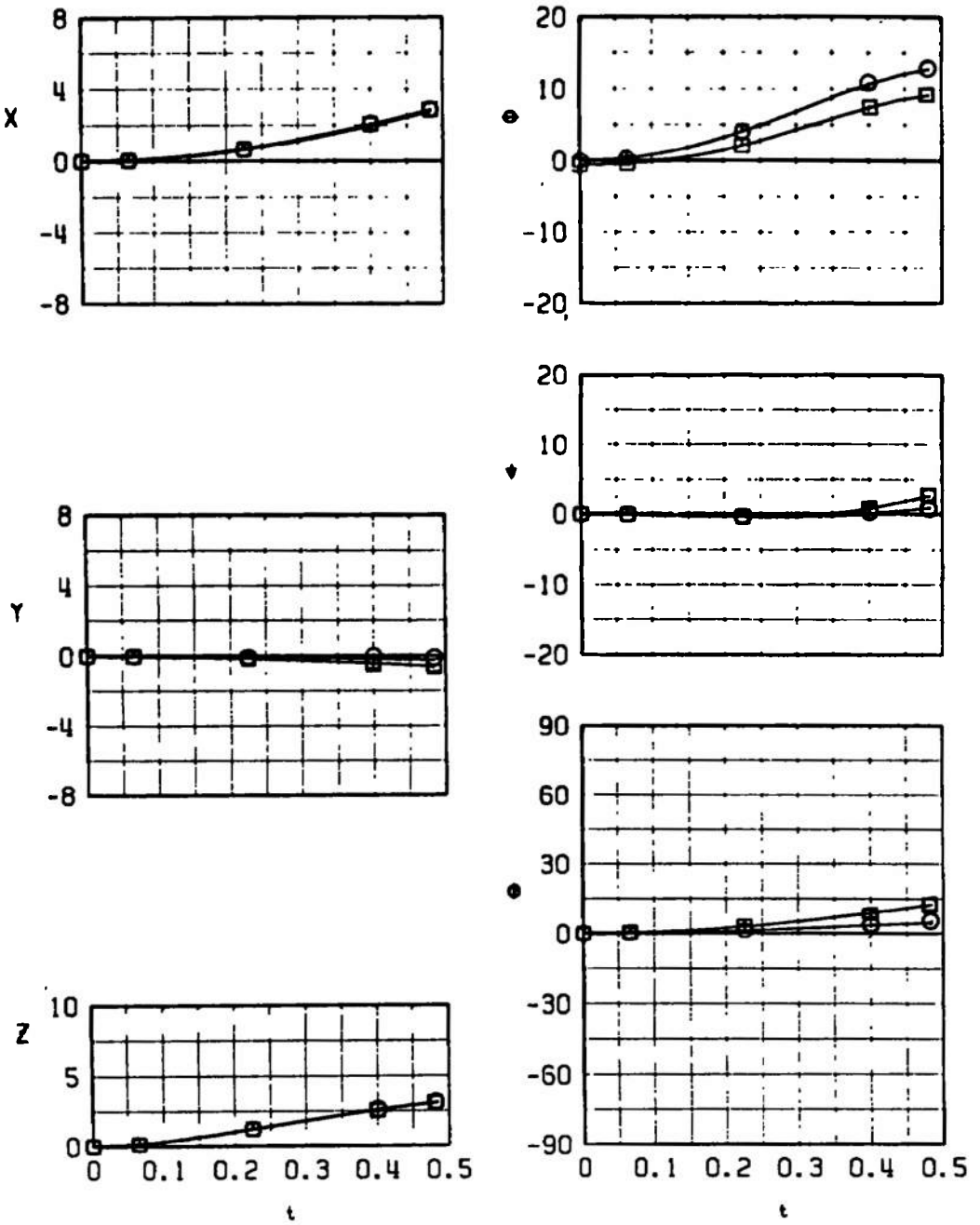

b. Configuration 12R
Fig. 25 Concluded

TABLE I
IDENTIFICATION OF SIMULATED EJECTOR FORCES

Identification No.	Store	Rack	Orifice Combination Simulated Forward/Aft	F_{Z_1}, lb	F_{Z_2}, lb	F_Z, lb
1	MK-84 LGB	MAU-12 B/A	No. 7/No. 5	2010	1700	---
2	MK-84 EOGB	MAU-12 B/A	↓	2030	1780	---
3	MK-82 LGB	MAU-12 B/A	↓	2110	1390	---
4	MK-82 LGB	MER	NA	---	---	1160
5	LAU-68 A/A (Expended)	TER	↓	---	---	1300
6	LAU-68 A/A (Loaded)	TER	↓	---	---	1220
7	BLU-1 Finned	MER	↓	---	---	1150

Note: Z_E = 0.24167 ft for the MER and TER

Z_E = 0.34167 ft for the MAU-12 B/A

TABLE II
FULL-SCALE STORE PARAMETERS USED IN TRAJECTORY CALCULATIONS

Parameter \ Store	MK-84 LGB	MK-84 EOGB	MK-82 LGB	LAU-68 A/A		BLU-1 Finned
				Expended	Loaded	
$\bar{m}$	64.006	70.342	18.789	2.081	5.932	22.405
X_{cg}	8.042	6.608	6.067	2.508	3.026	5.467
S	1.766	1.766	0.629	0.534	0.534	1.887
b	1.5000	1.5000	0.895	0.825	0.825	1.550
I_{xx}	24.00	25.000	2.000	0.400	1.0000	12.000
I_{yy}	416.00	525.00	79.000	4.6000	9.100	177.00
I_{zz}	416.00	525.00	79.000	4.6000	9.1000	177.00
C_{m_q}, C_{n_r}	-275.00	-110.00	-339.00	-31.100	-38.60	-48.000
C_{ℓ_p}	-20.00	-10.00	-19.600	0	0	-1.3000
X_L	---	---	-0.4500	0.2033	0.1200	-0.0833
X_{L_1}	0.592	0.592	0.558	---	---	---
X_{L_2}	-1.0750	-1.0750	-1.108	---	---	---
C_A	---	---	0.400	0.800	0.300	---

TABLE III
MAXIMUM FULL-SCALE POSITION UNCERTAINTIES
RESULTING FROM BALANCE INACCURACIES

Store	M_∞	t	Δx	Δy	Δz	$\Delta\theta$	$\Delta\psi$	$\Delta\phi$
MK-84 LGB	0.73	0.2	±0.005	±0.005	±0.005	±0.05	±0.05	±0.48
MK-84 EOGB	↓	↓	±0.004	±0.004	±0.004	±0.04	±0.04	±0.46
MK-82 LGB			---	±0.01	±0.01	±0.13	±0.13	±7.4
LAU-68 A/A (Loaded)			---	±0.03	±0.03	±1.1	±1.1	±14
LAU-68 A/A (Expended)			---	±0.09	±0.09	±2.3	±2.3	±36
BLU-1/B	0.80		±0.01	±0.01	±0.01	±0.09	±0.09	±0.75

TABLE IV
AIRCRAFT WING LOADING CONFIGURATION IDENTIFICATION

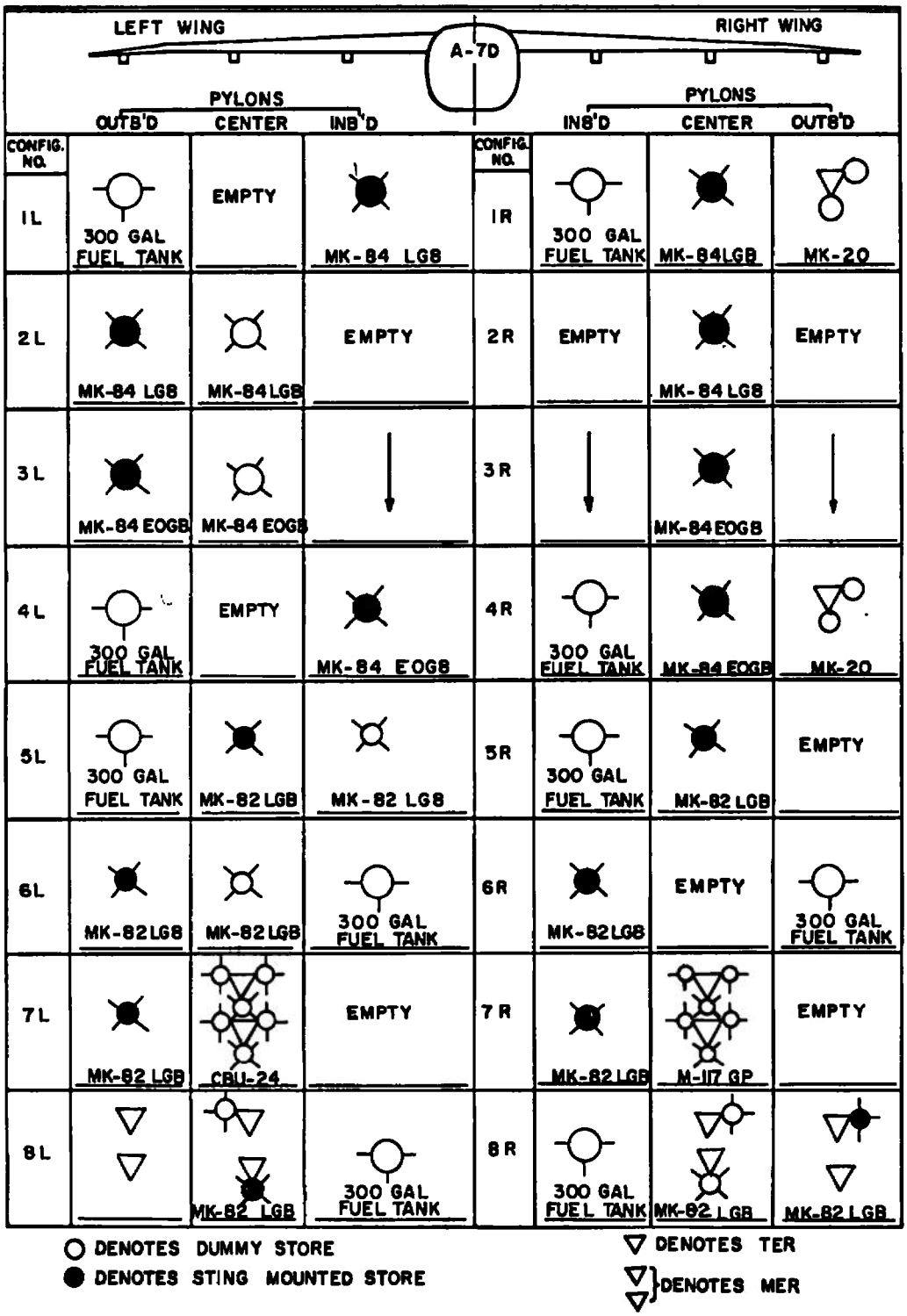

○ DENOTES DUMMY STORE

● DENOTES STING MOUNTED STORE

▽ DENOTES TER

▽▽ DENOTES MER

TABLE IV (Concluded)

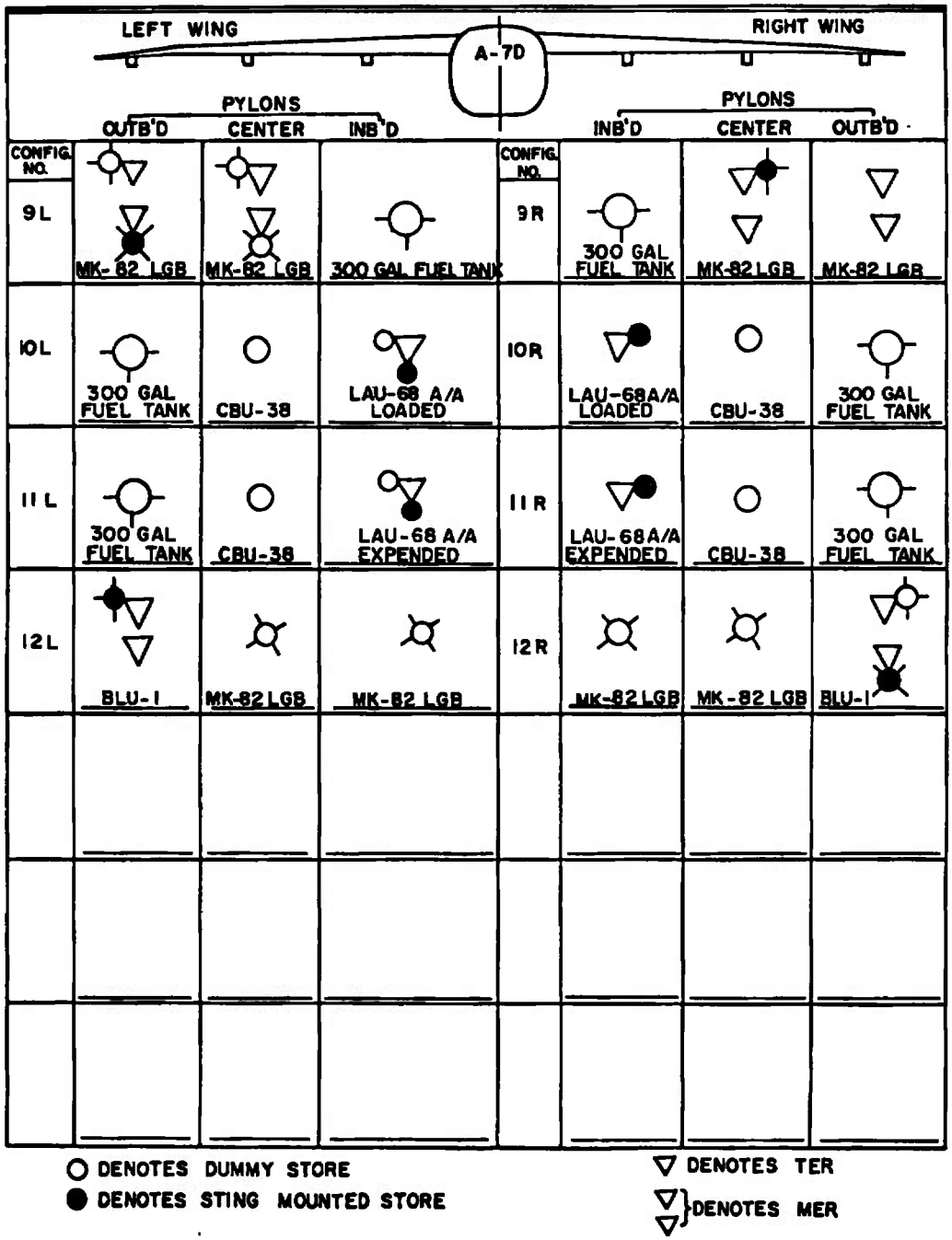

UNCLASSIFIED

Security Classification

DOCUMENT CONTROL DATA - R & D

(Security classification of title, body of abstract and indexing annotation must be entered when the overall report is classified)

1 ORIGINATING ACTIVITY (Corporate author)
Arnold Engineering Development Center
Arnold Air Force Station, Tennessee 37389

2a. REPORT SECURITY CLASSIFICATION
UNCLASSIFIED

2b. GROUP
N/A

3 REPORT TITLE

SEPARATION TRAJECTORIES OF VARIOUS MUNITIONS WHEN RELEASED FROM THE A-7D AIRCRAFT AT MACH NUMBERS FROM 0.33 TO 0.95

4 DESCRIPTIVE NOTES (Type of report and inclusive dates)
Final Report - September 22 to 28, 1972

5 AUTHOR(S) (First name, middle initial, last name)

David W. Hill, Jr., ARO, Inc.

6 REPORT DATE	7a. TOTAL NO OF PAGES	7b. NO OF REFS
February 1973	65	0

8a. CONTRACT OR GRANT NO	9a. ORIGINATOR'S REPORT NUMBER(S)
b. PROJECT NO	AEDC-TR-73-37 AFATL-TR-73-29
c. Program Element 27121F	9b. OTHER REPORT NO(S) (Any other numbers that may be assigned this report)
d. System 337A	ARO-PWT-TR-72-206

10 DISTRIBUTION STATEMENT Distribution limited to U.S. Government agencies only; this report contains information on test and evaluation of military hardware; February 1973; other requests for this document must be referred to Air Force Armament Laboratory (DLGC), Eglin AFB, FL 32542.

11 SUPPLEMENTARY NOTES	12 SPONSORING MILITARY ACTIVITY
Available in DDC	Air Force Armament Laboratory (DLGC) Eglin AFB, Florida 32542

13 ABSTRACT

Wind tunnel captive trajectory tests were conducted in the Aerodynamic Wind Tunnel (4T) to investigate the separation characteristics of various external stores from the wing, pylons, and racks of the A-7D aircraft. Separation trajectory data were obtained for the MK-84 LGB, M-84 EOGB, MK-82 LGB, and BLU-1/B bombs, and for the loaded and expended LAU-68 A/A rocket launcher. Trajectories were obtained at Mach numbers from 0.33 to 0.95 at simulated altitudes from 4,000 to 15,000 ft. At selected test conditions, parent-aircraft climb angles of 0 to -70 deg were simulated. In general, the stores separated from the aircraft without contacting the wing, pylon, or rack.

Distribution limited to U.S. Government agencies only; this report contains information on test and evaluation of military hardware; February 1973; other requests for this document must be referred to Air Force Armament Laboratory (DLGC), Eglin AFB, Florida 32542.

This document has been approved for public release and its distribution is unlimited. Per TAB 75-26 dtd 19Dec, 1975

DD FORM 1 NOV 65 1473

UNCLASSIFIED

Security Classification

14 KEY WORDS	LINK A		LINK B		LINK C	
	ROLE	WT	ROLE	WT	ROLE	WT
ammunition						
bombs						
A-7D aircraft						
separation						
trajectories						
transonic flow						
wind tunnel tests						
external stores						

AFSC
Arnold AFS Tenn